Superconducting quantum systems for dark matter search and cosmology

Federico Paolucci
Dipartimento di Fisica E. Fermi, Università di Pisa, Pisa, Italy
Istituto Nazionale di Fisica Nucleare, Sezione di Pisa, Pisa, Italy

Congresso di Dipartimento
27th May 2026

outline

scientific cases in astroparticle physics

superconducting detectors: state-of-the-art

our detection technologies

- nanoscale transition-edge sensor and Josephson escape sensor
- superconducting thermoelectric detector
- non-local superconducting detector

our devices in the technological landscape

people and fundings

scientific cases in astroparticle physics

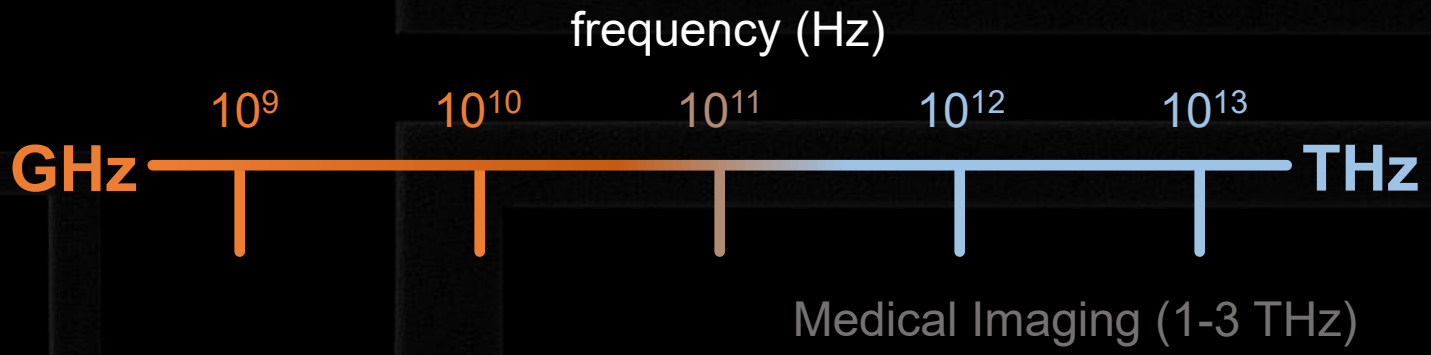

Medical Imaging (1-3 THz)

Phys. Rev. Lett. **78**, 2054 (1997)
Science **325**, 546 (2009)
Phys. Dark Univ. **12**, 37 (2016)
FP, et al., Phys. Rev. Appl. **14**, 034055 (2020)
FP, et al., J. Appl. Phys. **128**, 194502 (2020)
FP, et al., Appl. Sci. **11**, 746 (2021)
FP, et al., Instruments **5**, 14 (2021)
FP, et al., Instruments **8**, 47 (2024)

Dark Matter (1 GHz- 10 THz) single photons of energy 1-100 meV

Cosmic Microwave Barckground (0.3-630 GHz) e.m. signals of power 10 fW – 100 pW

Search of drugs and explosives (1-3 THz)

Safety imaging (100-300 GHz)

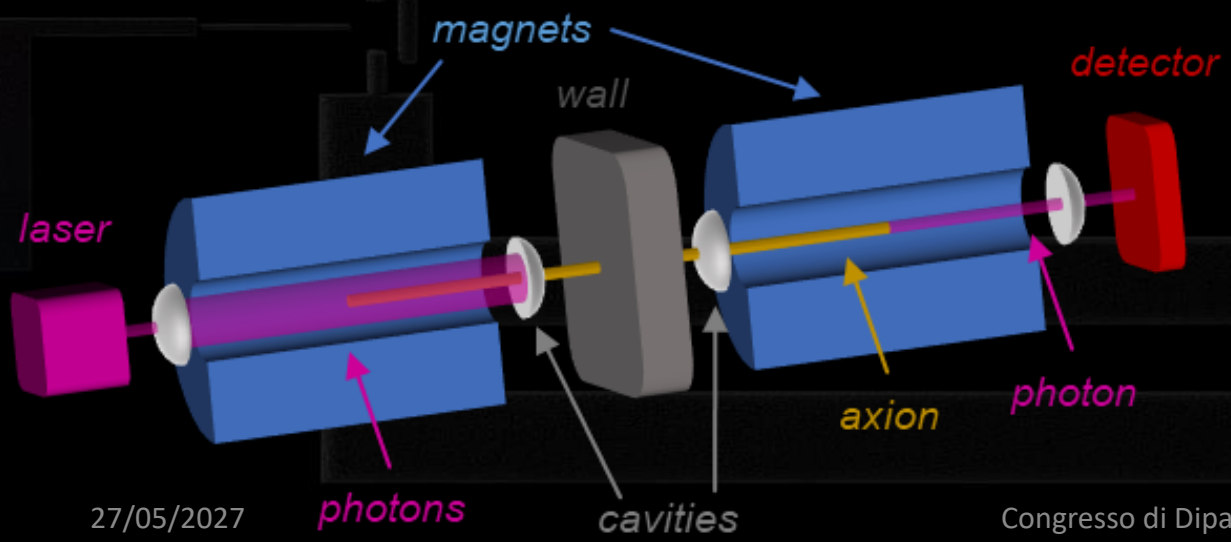

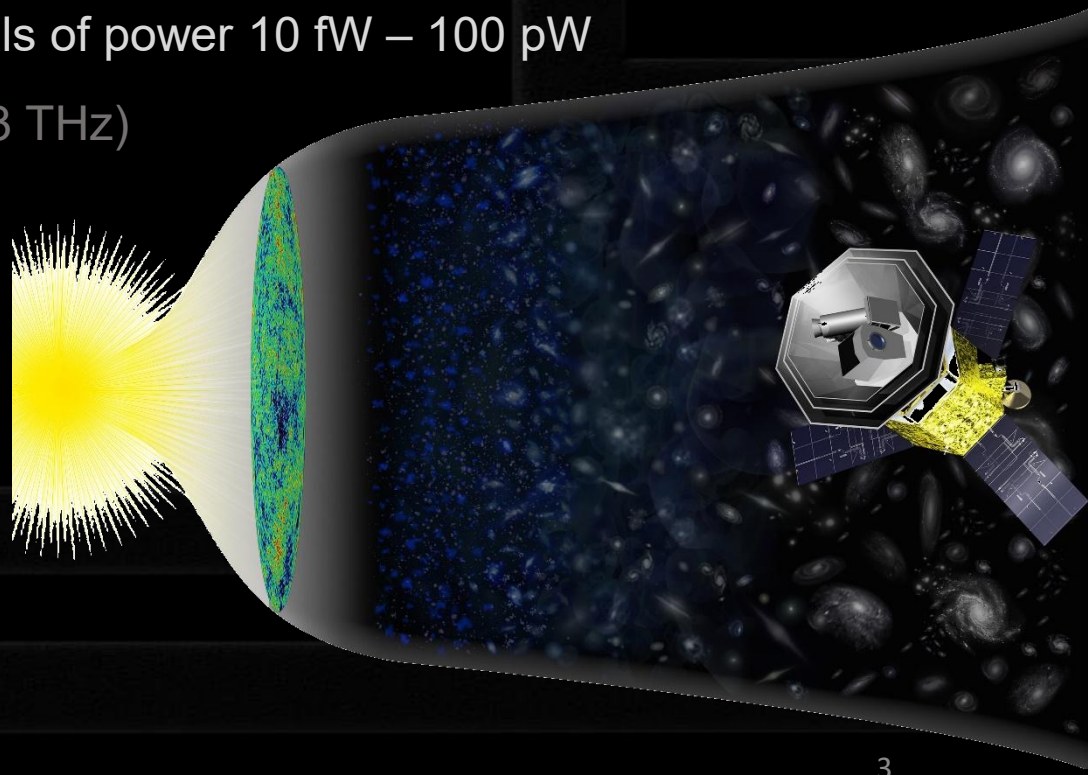

superconducting detectors: state-of-the-art

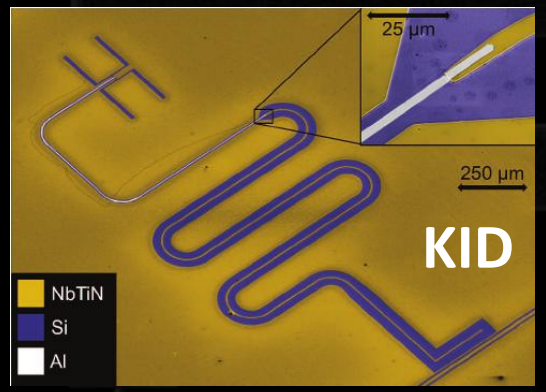

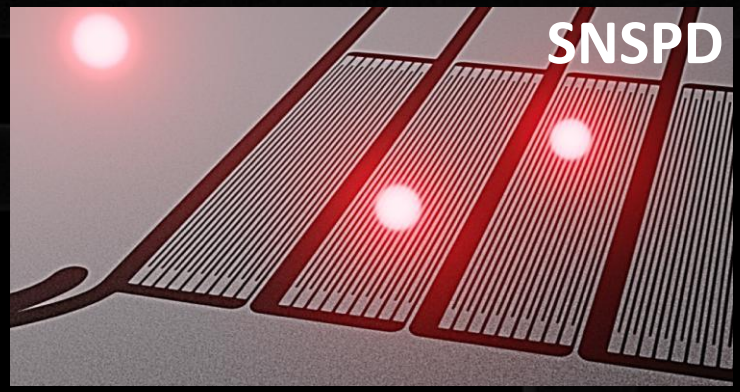

Detector	TES	KID	SNSPD	CEB	qubit
NEP ($WHz^{-1/2}$)	10^{-19}	10^{-18}	NO	10^{-18}	NO
Freq. Res. (Hz)	$5x10^{11}$	$5x10^{11}$	NO (10^{11})	NO	NO (10^{9})

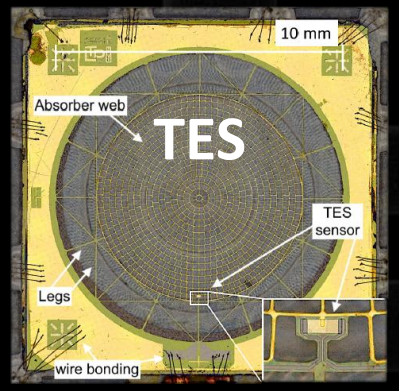

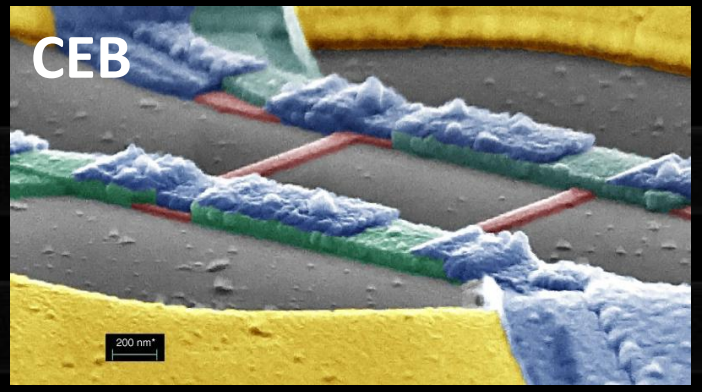

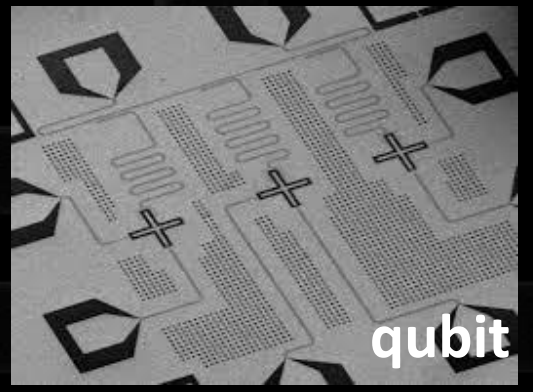

our detection technologies

nanoscale transition-edge sensor and Josephson escape sensor

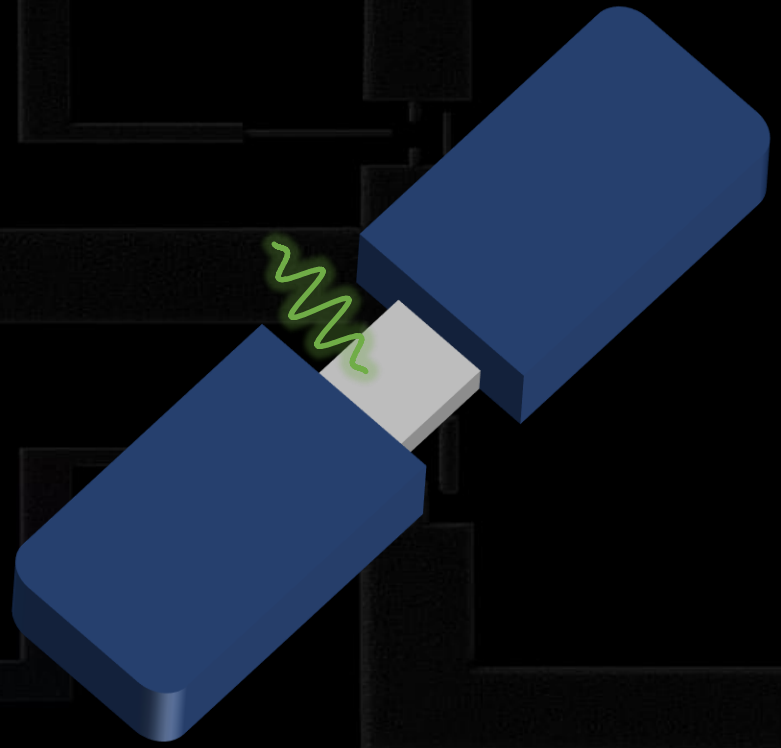

FP, et al., J. Appl. Phys. **128**, 0021996 (2020)
FP, NL, VB, GG, PV, FG, Phys. Rev. Appl. **14**, 034055 (2020)
FP, et al., IPN: WO2023062603A1), WIPO-PCT (20/04/2023)

superconducting thermoelectric detector

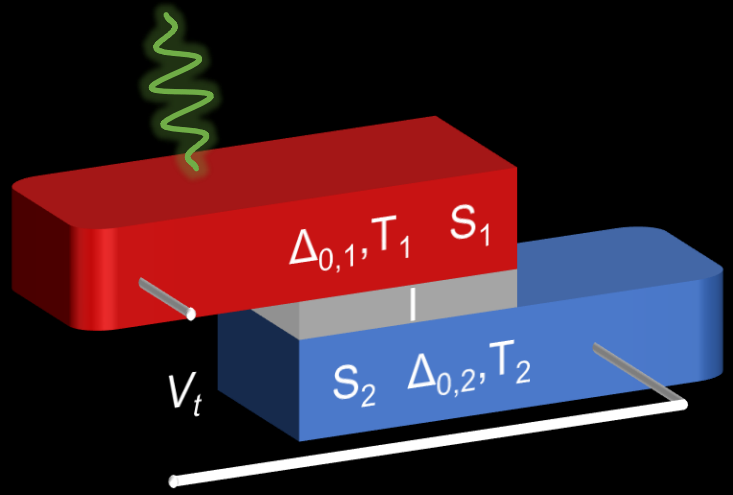

GG, **FP**, et al, Nat. Nanotech. **17**, 1084 (2022)
FP, et al., Appl. Phys. Lett. **122**, 173503 (2023)
FP, et al., FN: 102021000032042, UIB (2023)

non-local superconducting detector

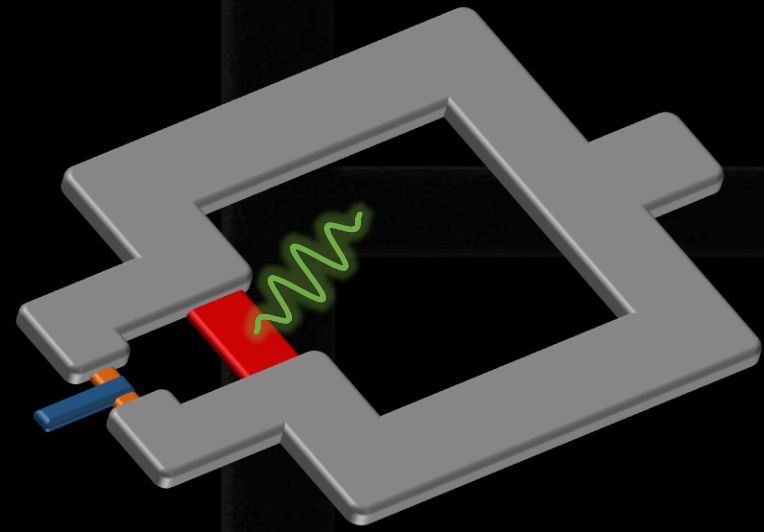

FP, Phys. Rev. Appl. **20**, 014003 (2023)

nanoscale transition-edge sensor (nano-TES)

and

Josephson escape sensor (JES)

nano-TES: basics

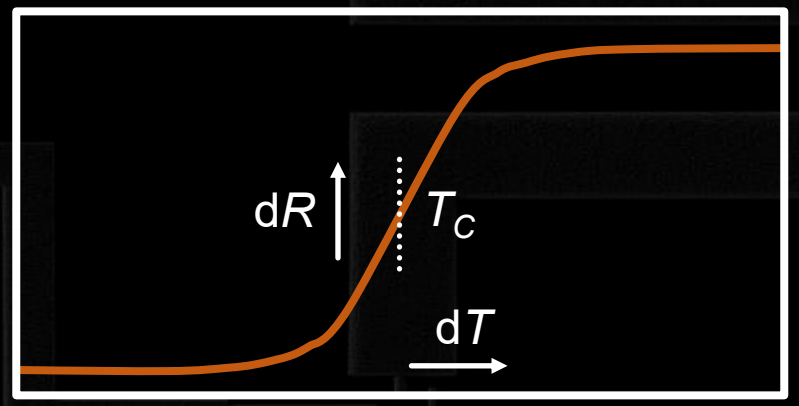

figure of merit $\alpha = \frac{T}{R}\frac{dR}{dT}$

only electron-phonon thermalization

$\dot{Q}_{e-ph} = \Sigma\mathcal{V}\left(T_e^5 - T_{bath}^5\right)$

Σ: scattering constant

$\mathcal{V}$: volume

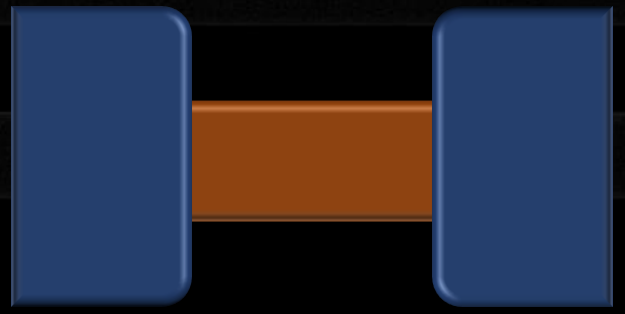

active region: 2D superconductor
superconducting electrodes

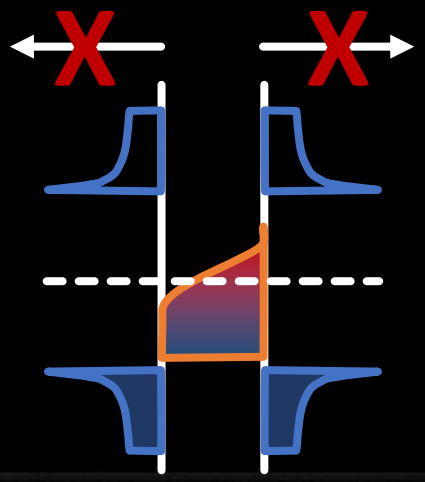

$\Delta_{el} > \Delta_{ar}$

no electrical resistance

no thermal leaks

absorbed power/energy

↓

temperature increase

↓

change of resistance

↓

system out-of-equilibrium

nano-TES: basics

$$\dot{Q}_{\mathrm{e-ph}} = \dot{Q}_{\upsilon} + \dot{Q}_{J} = \text{constant}$$

$$\dot{Q}_{J} = VI$$

the TES works at constant voltage

measurement of current variations

$$\delta\dot{Q}_{\upsilon} = -\delta\dot{Q}_{J}$$

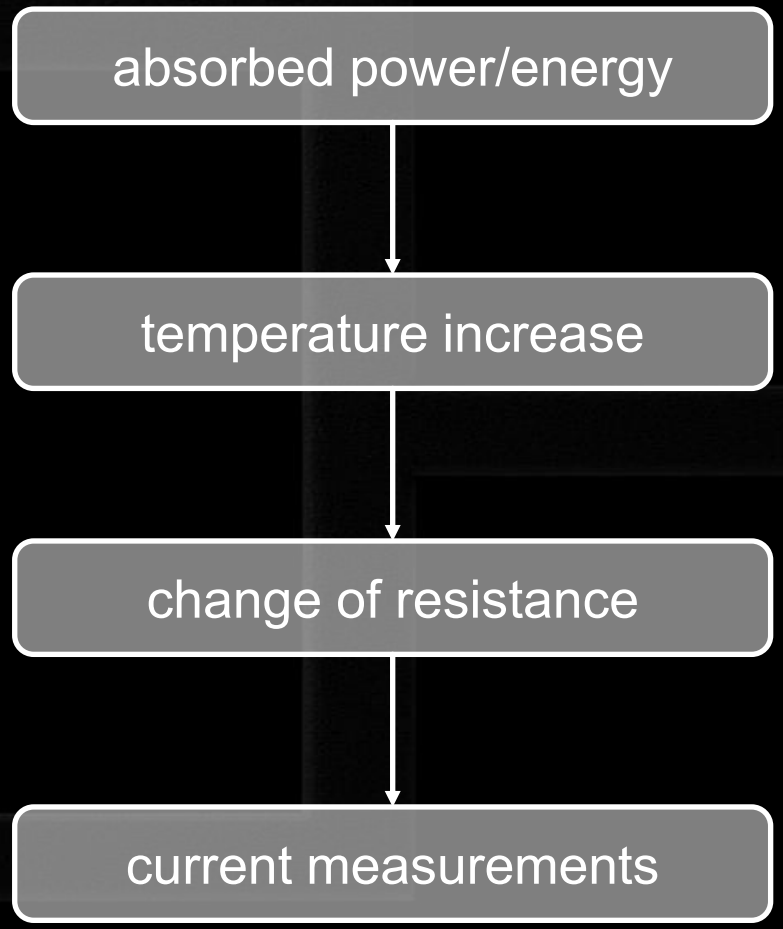

Appl. Phys. Lett., **66**, 1998 (1995)

JES: basics

System:

1D fully superconducting Josephson junction

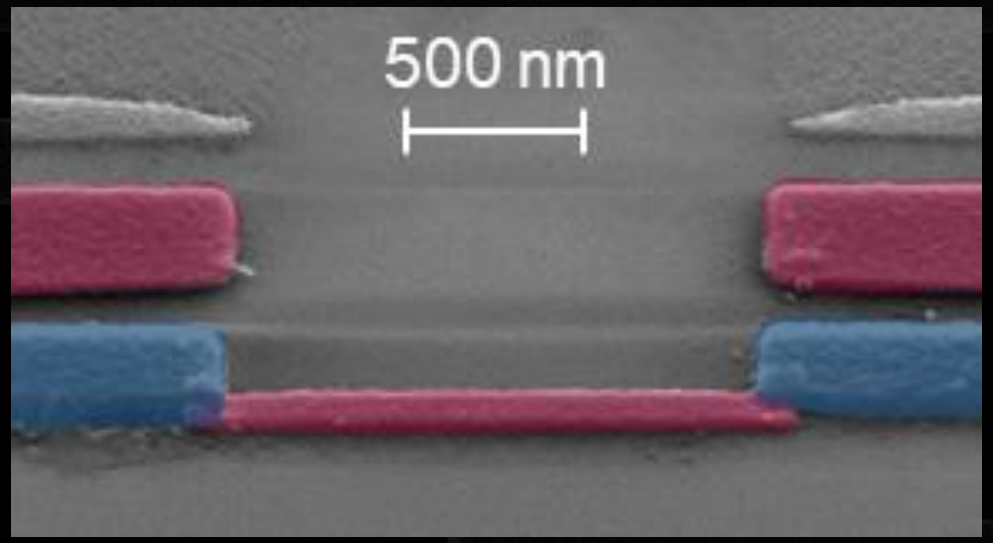

Quantum-mechanical effect:

Current-driven de-phasing to tune T_C

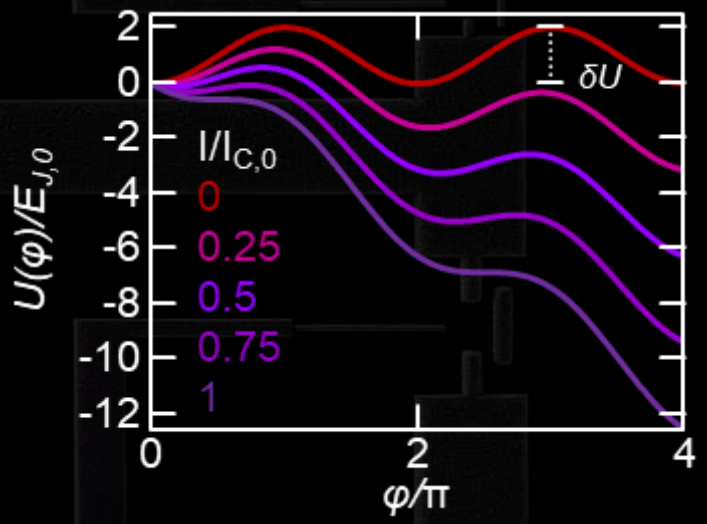

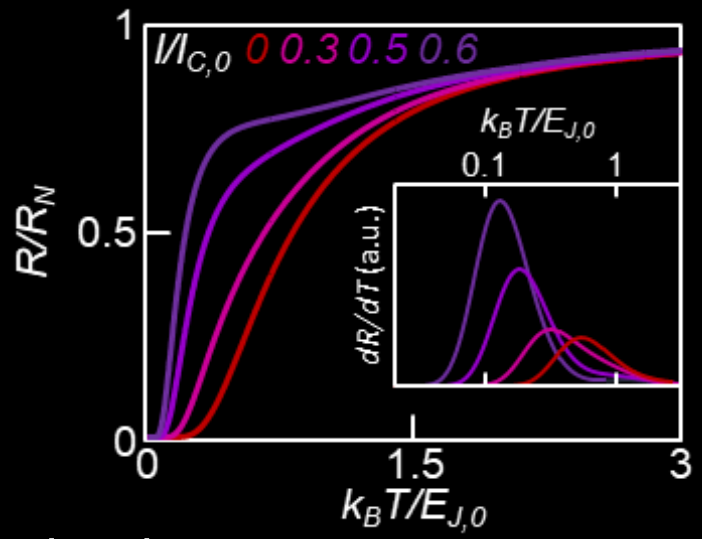

escape barrier

$$\delta U(I, E_J) \sim 2E_J(1 - I/I_{C,0})^{5/4}$$

1D Ivanchenko Zil'berman

$$V(I, E_J, T) = R_N \left(I - I_{C,0} \operatorname{Im} \frac{\mathcal{J}_{1-iz}\left(\frac{E_J}{k_B T}\right)}{\mathcal{J}_{-iz}\left(\frac{E_J}{k_B T}\right)} \right)$$

E_J: Josephson energy

$I_{C,0}$: zero-temperature critical current

FP, NL,VB, GG, PV, FG, Phys. Rev. Appl. **14**, 034055 (2020)

FP, NL, GG, FP, IPN: WO2023062603A1), WIPO-PCT (20/04/2023)

Sov. Phys. JETP **28**, 1272 (1969)

JES: expected performance

System:
1D fully superconducting Josephson junction

Quantum-mechanical effect:
Current-driven de-phasing to tune T_C

NEP:
~10^{-23} W/Hz$^{1/2}$

Energy resolution:
1 GHz

Advantages:
tunable sensitivity and *T*
same read-out of TES

Best applications:
polarization of CMB
dark matter

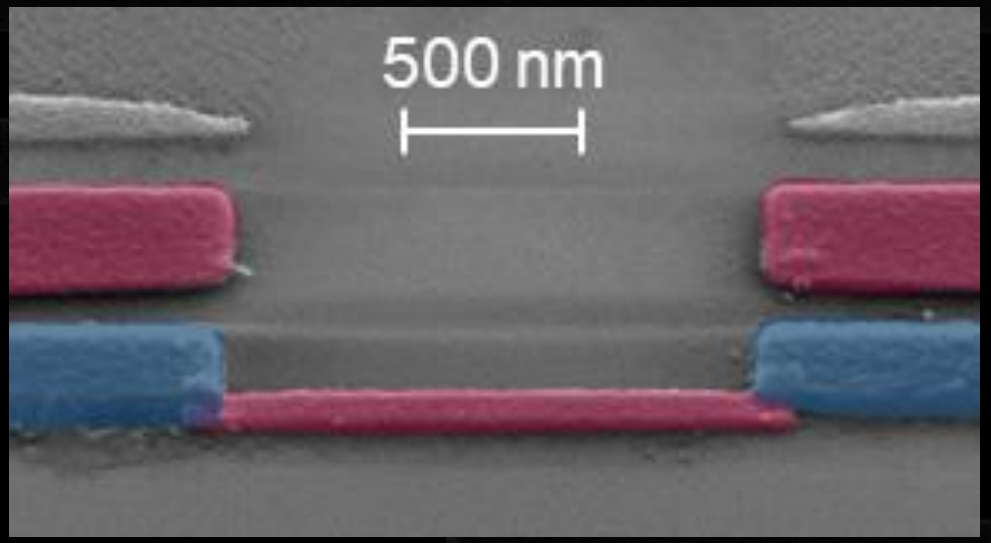

bolometer

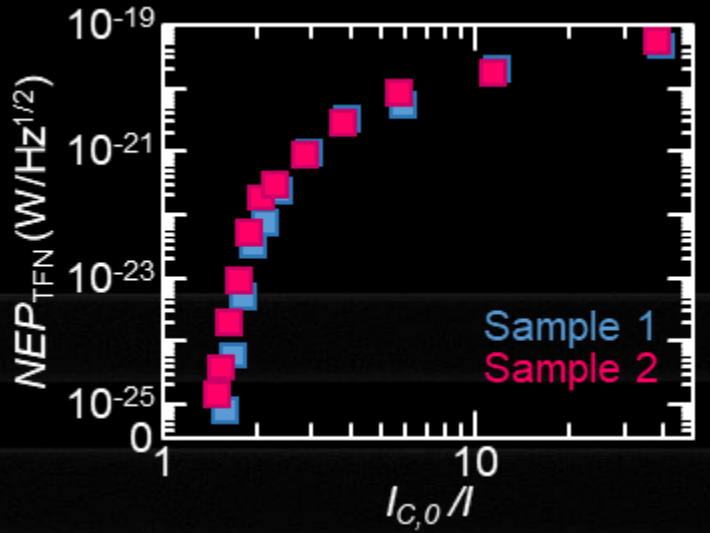

calorimeter

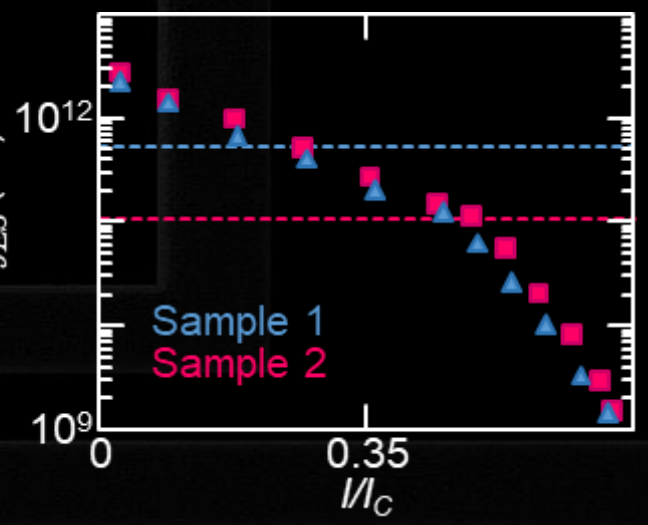

FP, NL,VB, GG, PV, FG, Phys. Rev. Appl. **14**, 034055 (2020)
FP, NL, GG, FP, IPN: WO2023062603A1), WIPO-PCT (20/04/2023)

TES/JES: ongoing activities

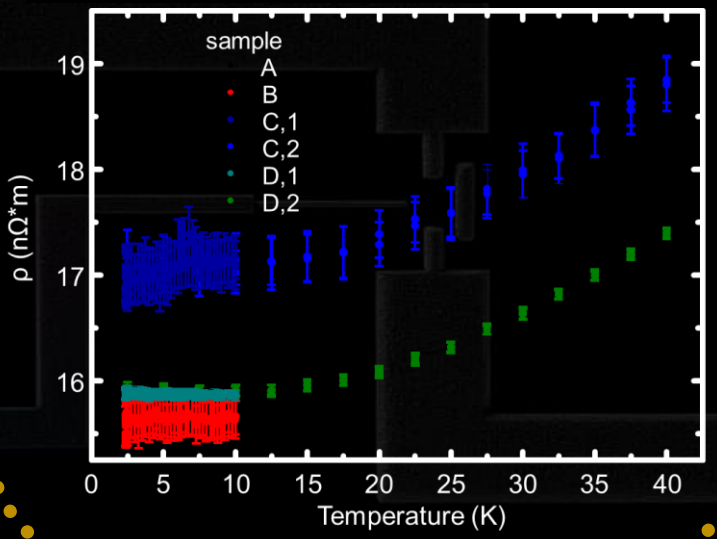

Au shunt resistor

low temperature resistivity

diffusion constant

coherence length

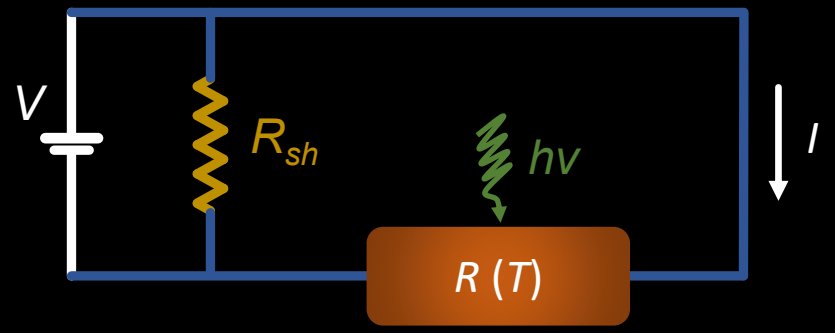

Nb superconducting electrodes

T_S and T_N vs width and thickness

impact of oxygen from PMMA

critical dimensions for TES/JES

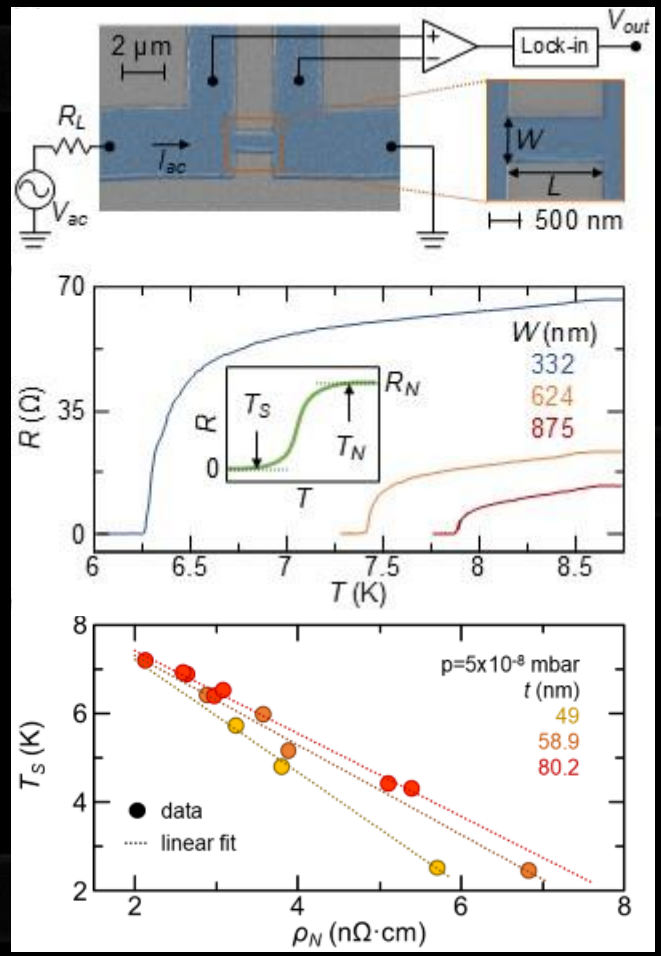

AK, FS, PS, DC, RB, FC, CP, GDS, FB, **FP**, arXiv:2603.24379 (2026)

TES/JES: ongoing activities

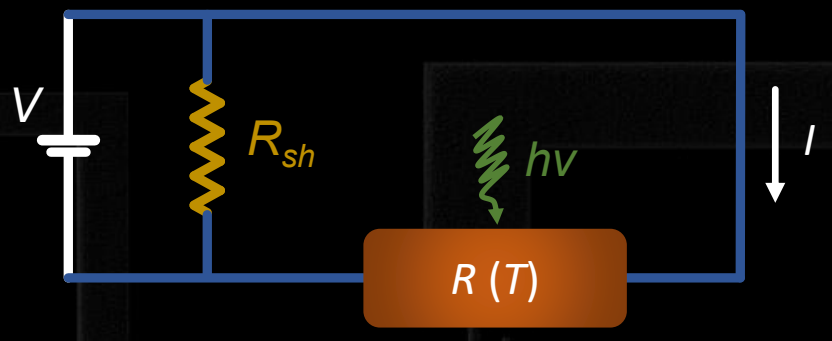

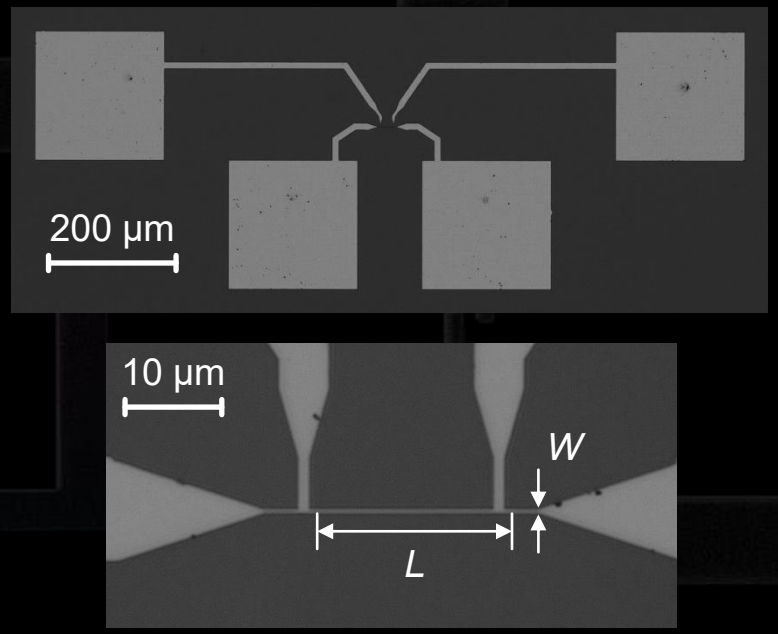

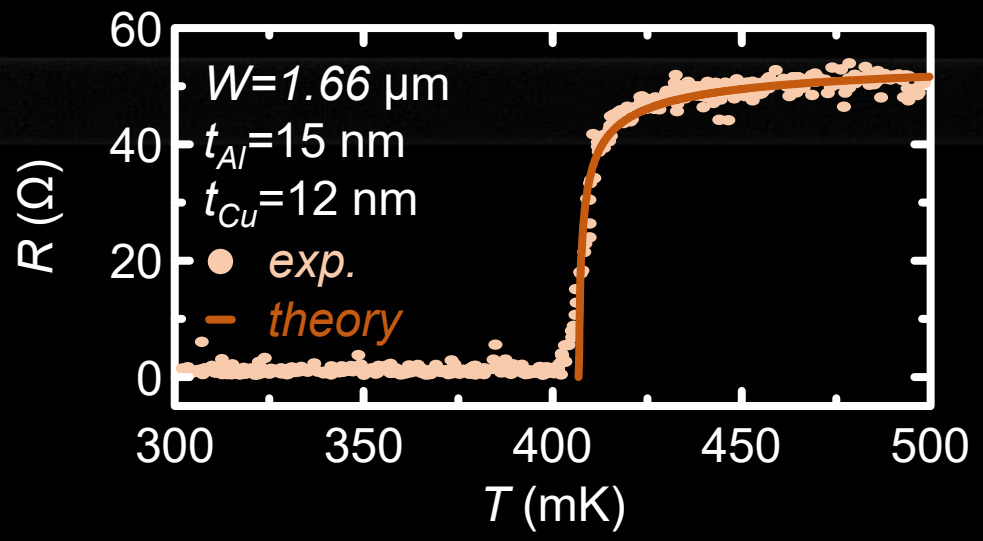

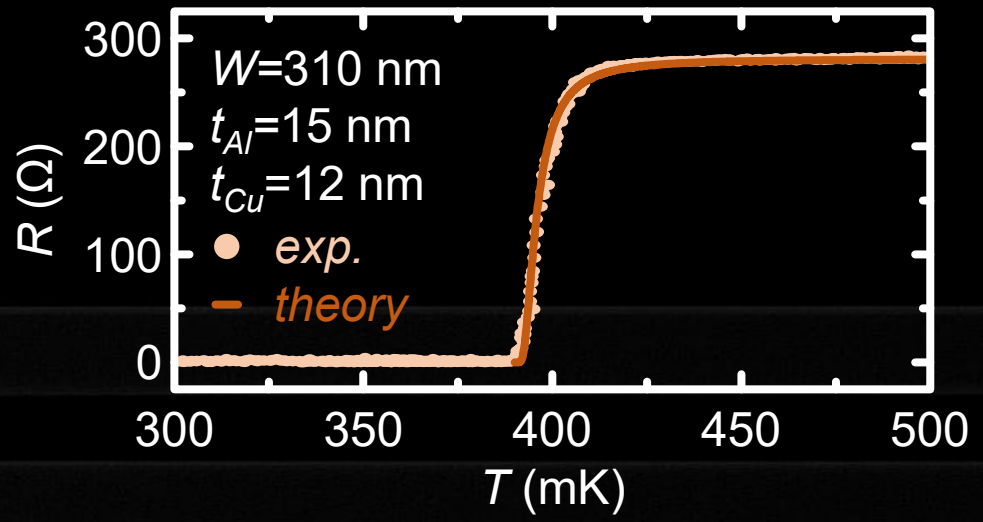

2D BKT

$$R(T) = R_0\, e^{-b\sqrt{\frac{T_{BKT}}{T}}}$$

R_0 : effective BKT temperature

b: core vortex parameter

T_{BKT}: BKT transition temperature

J. Low Temp. Phys. **36**, 599–616 (1979)

J. Phys. C: Solid State Physics **6**,1181 (1973)

1D Ivanchenko Zil'berman

$$V(I, E_J, T) =$$

$$R_N \left(I - I_{C,0}\, \mathrm{Im} \frac{\mathcal{I}_{1-iz}\left(\frac{E_J}{k_B T}\right)}{\mathcal{I}_{-iz}\left(\frac{E_J}{k_B T}\right)} \right)$$

E_J: Josephson energy

$I_{C,0}$: zero-T critical current

Sov. Phys. JETP **28**, 1272 (1969)

AK, RB, FC, CP, AT, GL, GS, **FP**, in preparation

superconducting thermoelectric detector (STD)

STD: physics background

Sufficient and universal conditions for finite thermoelectric power ($IV<0$)

- Tunnel junction between two particle-hole symmetric systems
- Large temperature gradient (δT~T/2, non-linear response regime)
- The hot electrode has a gapped DOS
- The cold electrode has a locally monotonically decreasing DOS

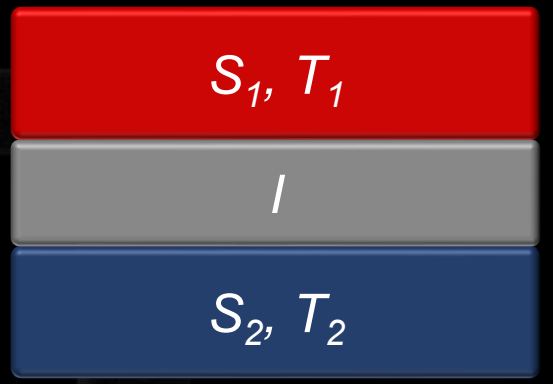

spontaneous particle-hole symmetry breaking

Prototypical example: tunnel junction between two different superconductors
quasiparticles transport (no Josephson effect)

$$I_{qp} = \frac{1}{eR_T}\int_{-\infty}^{\infty} d\epsilon N_1(\epsilon)N_2(\epsilon + eV)[f_0(\epsilon, T_1) - f_0(\epsilon + eV, T_2)]$$

$$N_i(\epsilon, T_i) = \left|\Re\left[\frac{(\epsilon + i\Gamma_i)}{\sqrt{(\epsilon + i\Gamma_i)^2 - \Delta_i(T_i)^2}}\right]\right|$$

$$f_0(\epsilon, T_i) = [1 + \exp(\epsilon/k_B T_i)]^{-1}$$

Phys. Rev. Lett. **124**, 106801 (2020)

STD: physics background

$r = \Delta_{0,2}/\Delta_{0,1} < 0.85$

$k_B T_2 << \Delta_1(T_1)$

$$I_{qp} \sim \frac{1}{eR_T}\int_{-\infty}^{\infty} d\epsilon N_1(\epsilon)[N_2(\epsilon + eV) - N_2(\epsilon - eV)]f_0(\epsilon, T_1)$$

$V \sim 0$

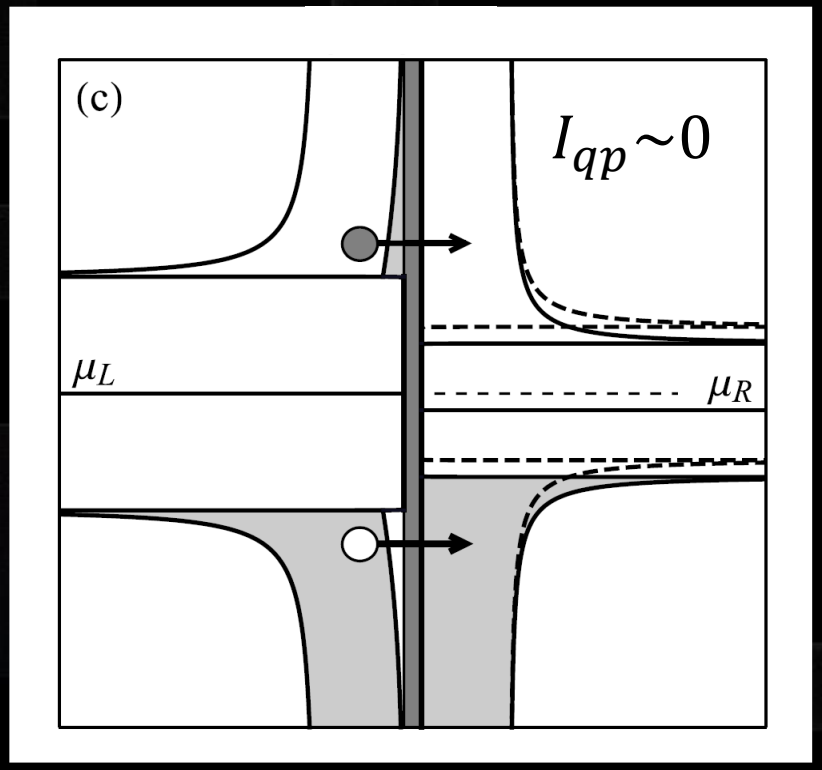

$eV \sim \Delta_1(T_1) - \Delta_2(T_2)$

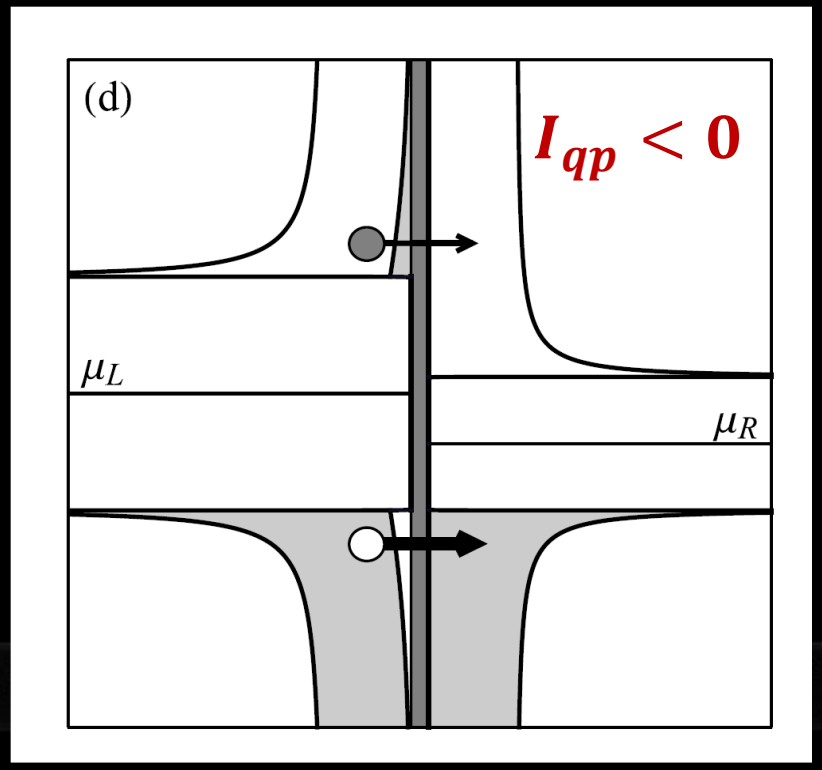

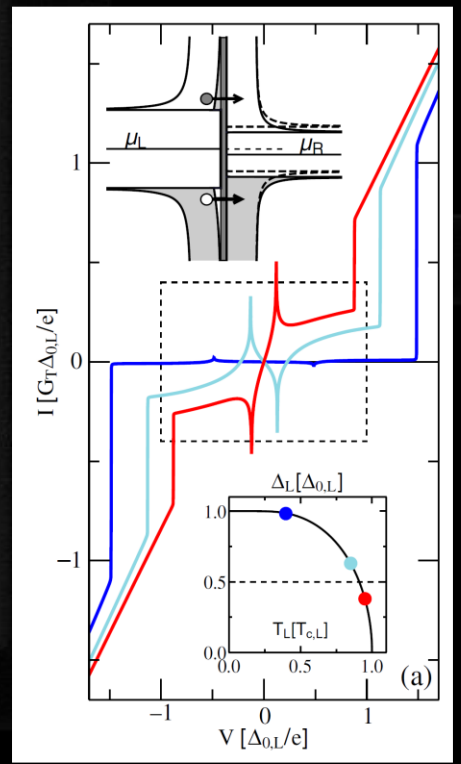

Phys. Rev. Lett. **124**, 106801 (2020)
Phys. Rev. B **101**, 214509 (2020)

spontaneous particle-hole symmetry breaking

STD: physics background

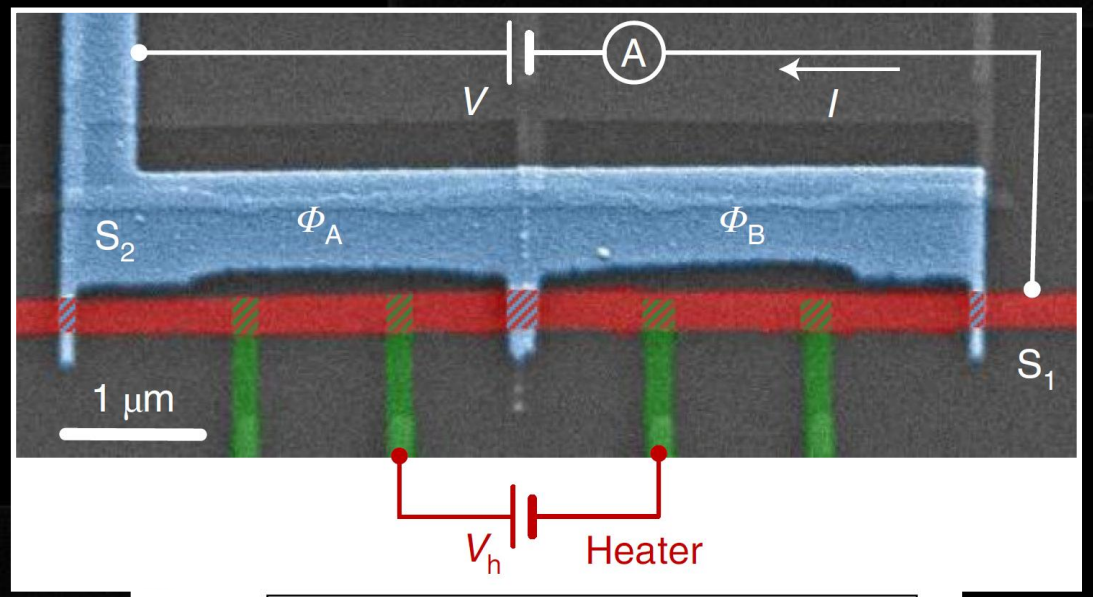

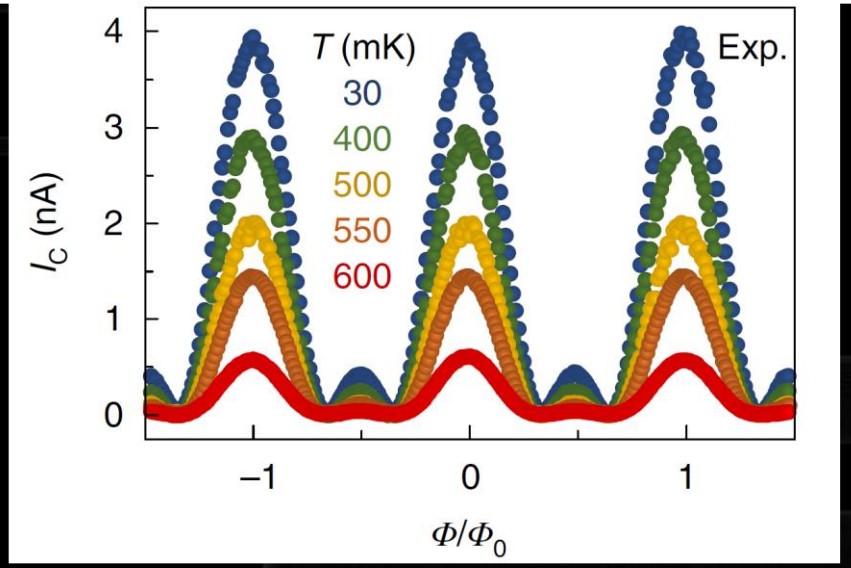

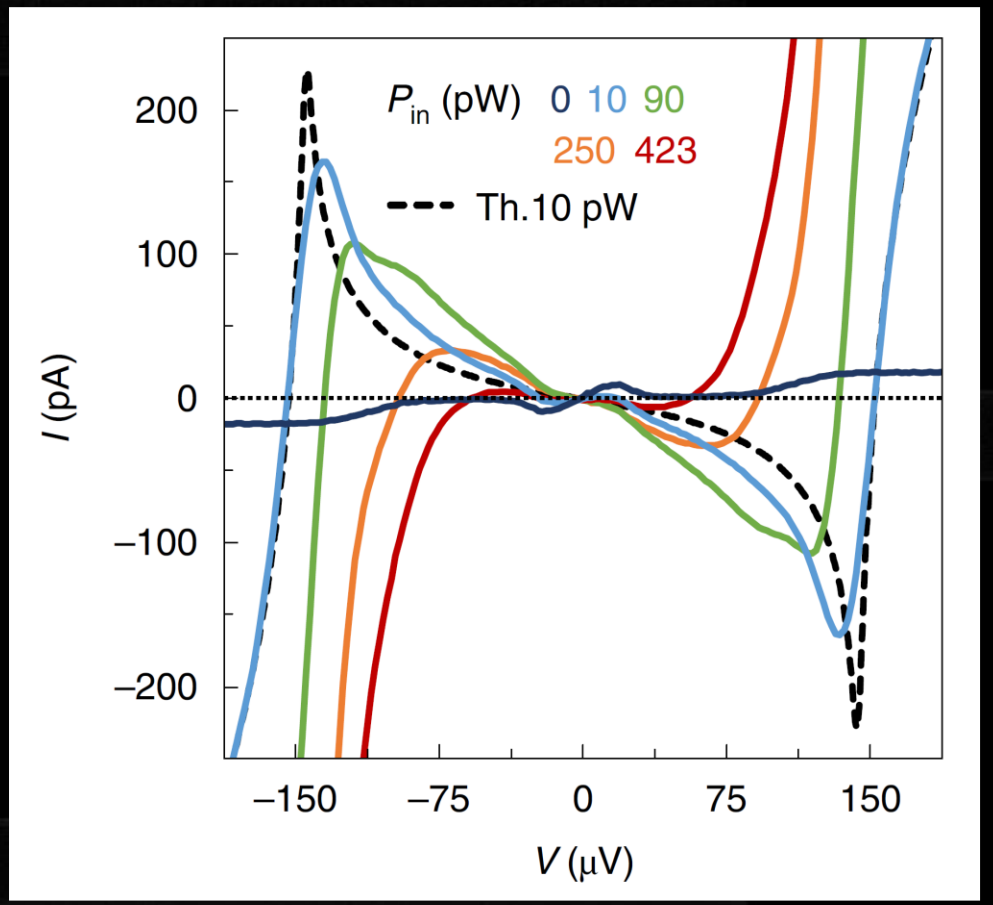

GG, **FP**, et al, Nat. Nanotech. **17**, 1084 (2022)

STD: physics background

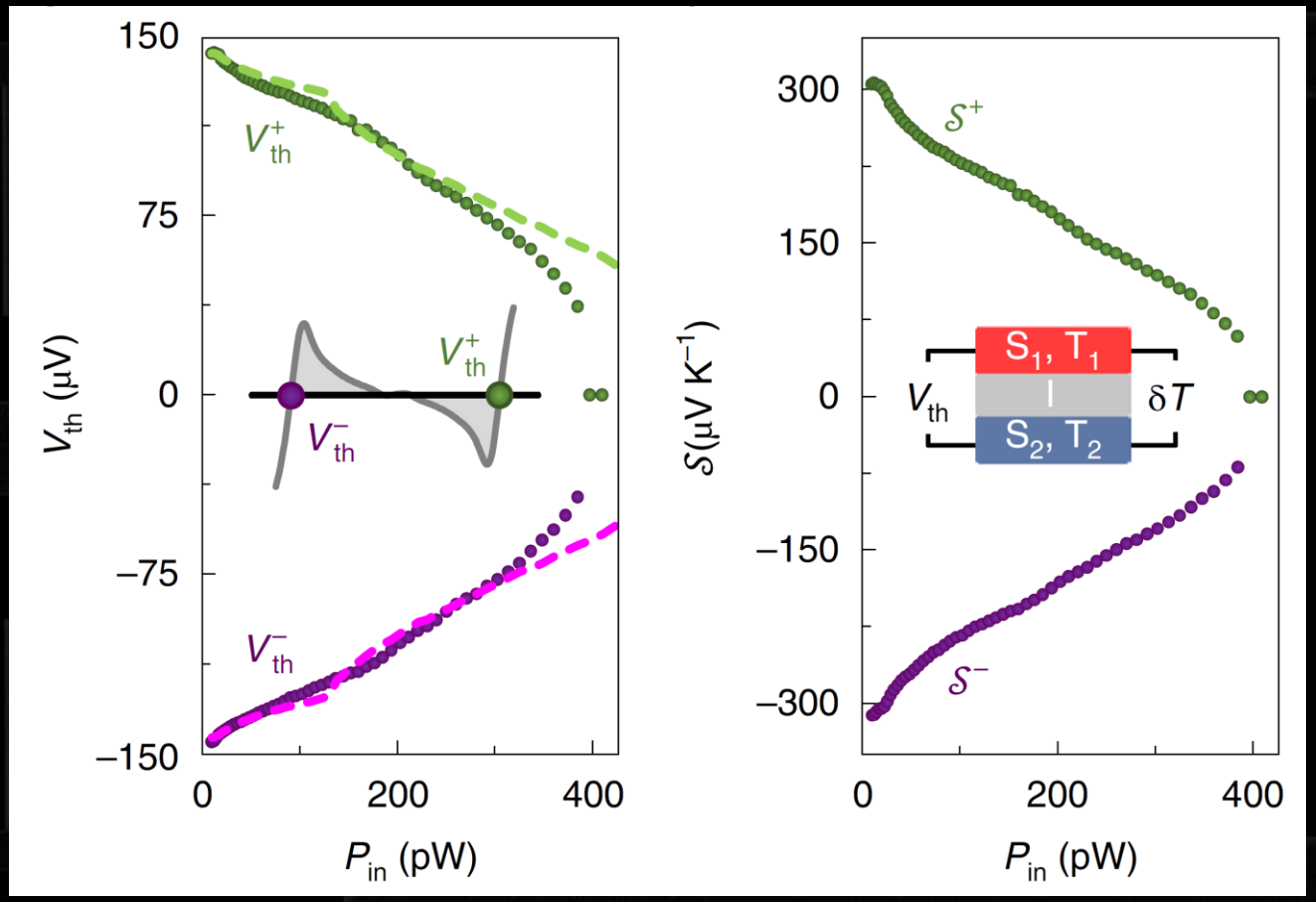

non-linear Seebeck coefficient

$$\mathcal{S} = \frac{V_{th}}{\delta T} \cong 300\ \mu\mathrm{VK}^{-1}$$

linear Seebeck coefficient for aluminium
Mott-Jones equation

$$\mathcal{S}_{Al}(T = 600\ \mathrm{mK}) = \left(\frac{\pi^2 k_B^2 T}{3eE_{F,0}}\right) \cong -3.8\ \mathrm{nVK}^{-1}$$

larger than semiconductors and comparable to quantum dots at cryogenic temperatures

GG, **FP**, et al, Nat. Nanotech. **17**, 1084 (2022)
The Theory of the Properties of Metals and Alloys (Dover Publications, 1958)

STD: expected performance

System:

S_1IS_2 tunnel junction

Quantum-mechanical effect:

quantum tunneling

thermoelectricity in e-h symmetric systems

NEP:

ongoing

Energy resolution:

1 GHz

Advantages:

large bandwidth (10^{10}-10^{16} Hz)

passive detector

Best applications:

balloon or satellite experiments

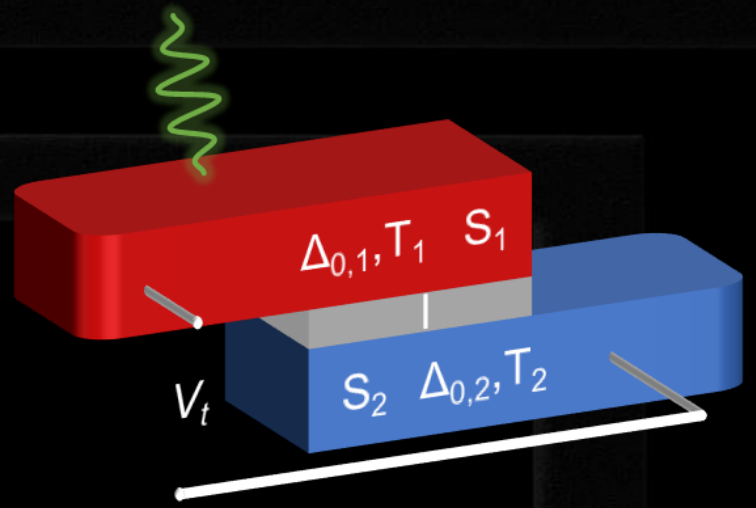

Time constant **Signal-to-noise ratio**

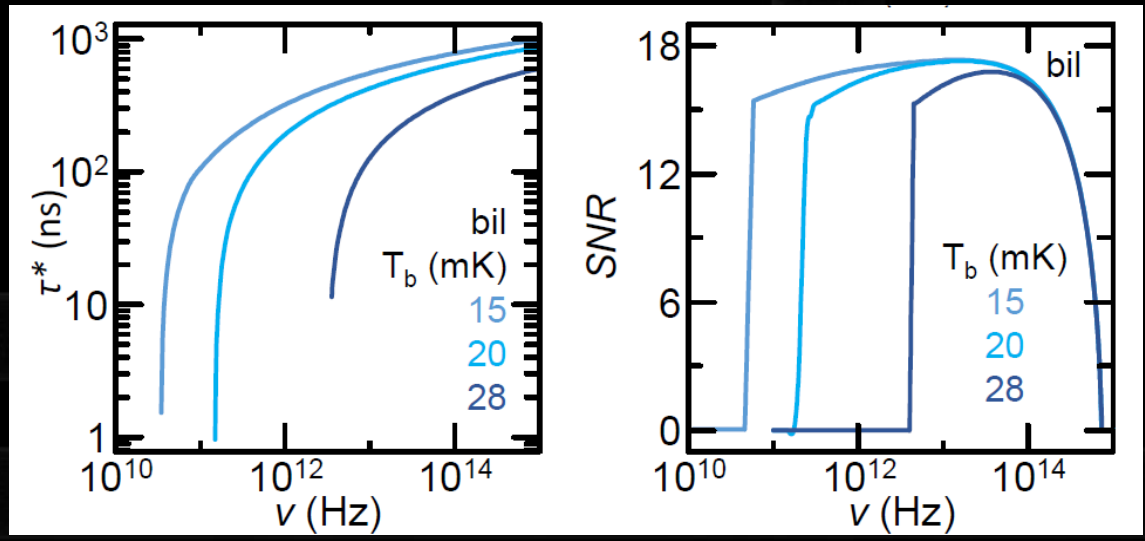

GG, **FP**, et al, Nat. Nanotech. **17**, 1084 (2022)

FP., et al., Appl. Phys. Lett. **122**, 173503 (2023)

FP, et al., FN: 102021000032042, Ufficio Italiano Brevetti (2023)

STD, ongoing activities: SIG

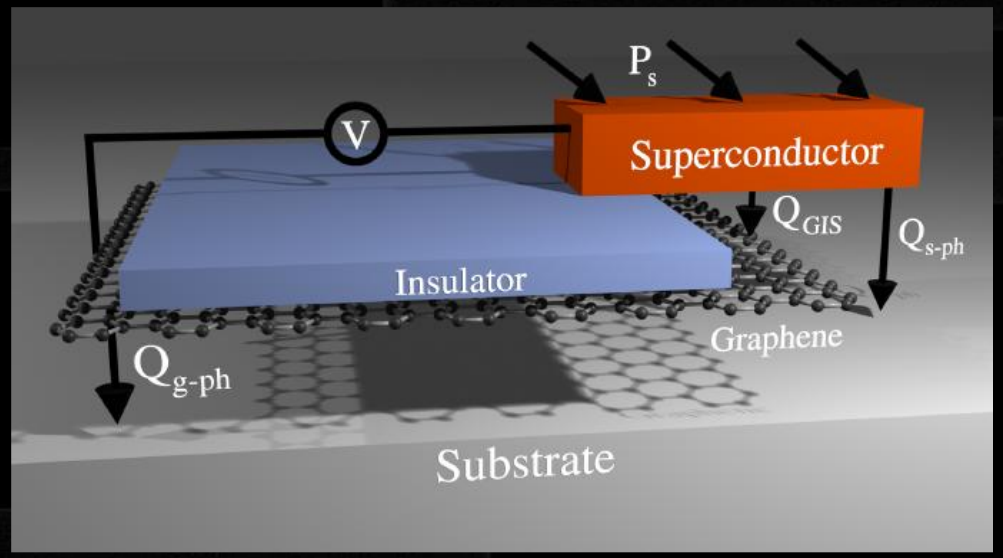

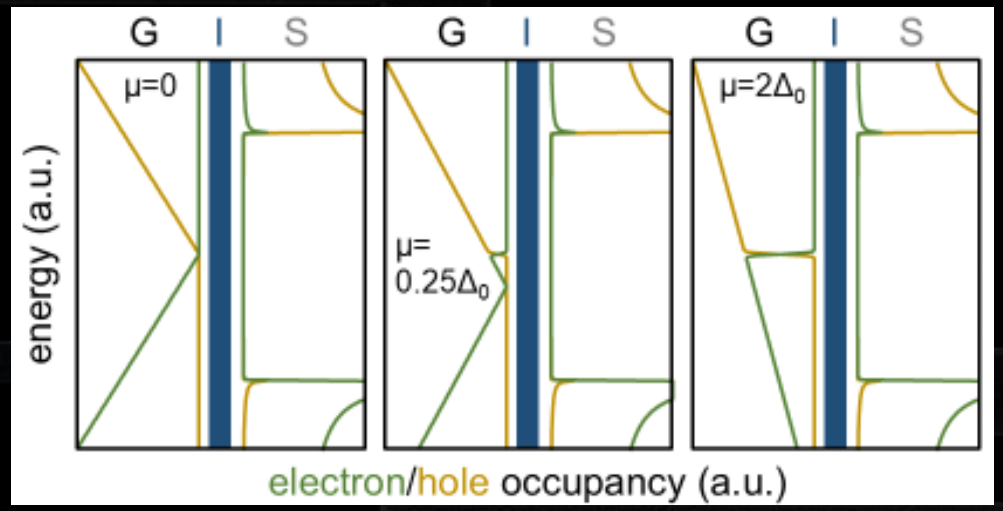

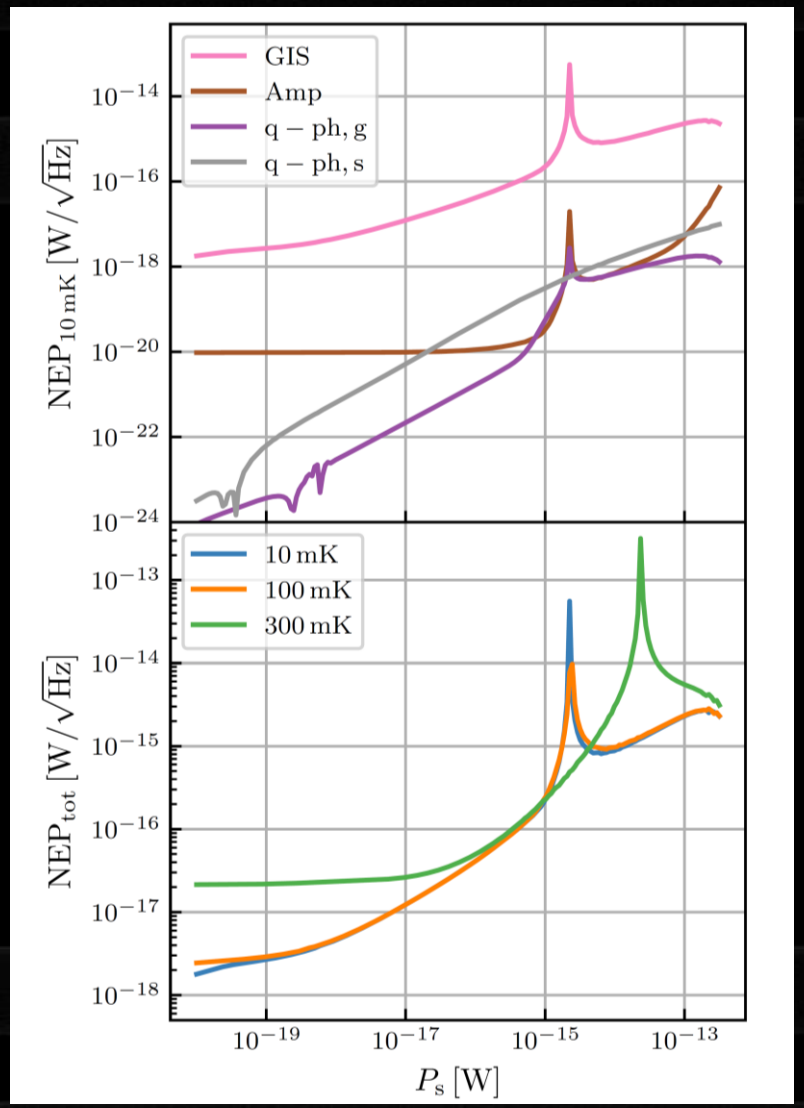

System:

SIG

NEP:

~10^{-18} W/Hz$^{1/2}$

Energy resolution:

ongoing

Time constant:

10^{-6} s

No Josephson coupling

Need of non-linear model

FB, DZ, **FP**, J. Appl. Phys. **136**, 154901 (2024)
LL, **FP**, Phys. Rev. B **112**, 184509 (2025)

FP, FB, FG, SR, Adv. Funct. Mater. **35**, 2418456 (2025)
LL, **FP**, arXiv:2512.14493(2025), accepted in Phys. Rev. Appl.

STD, ongoing activities: SI2DEG

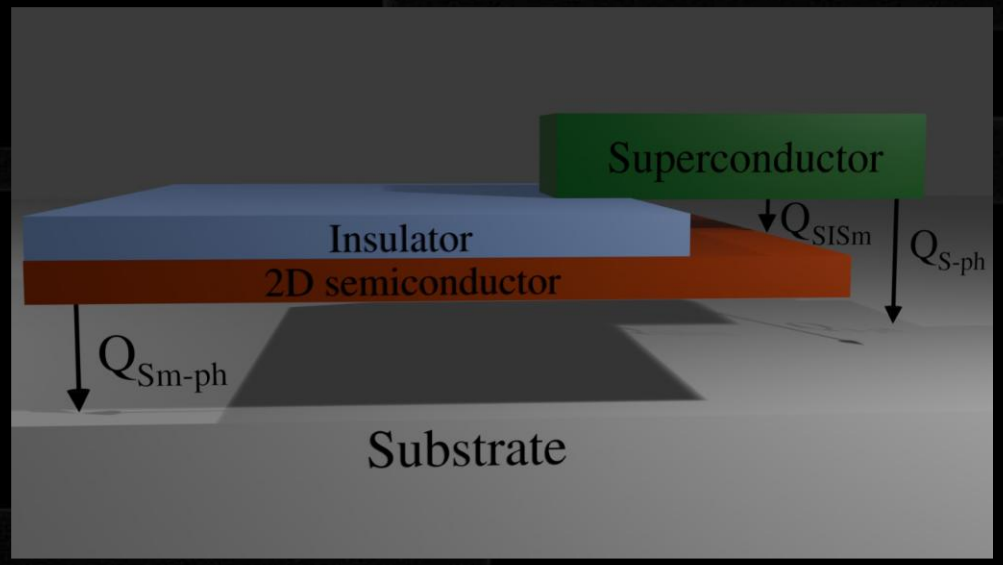

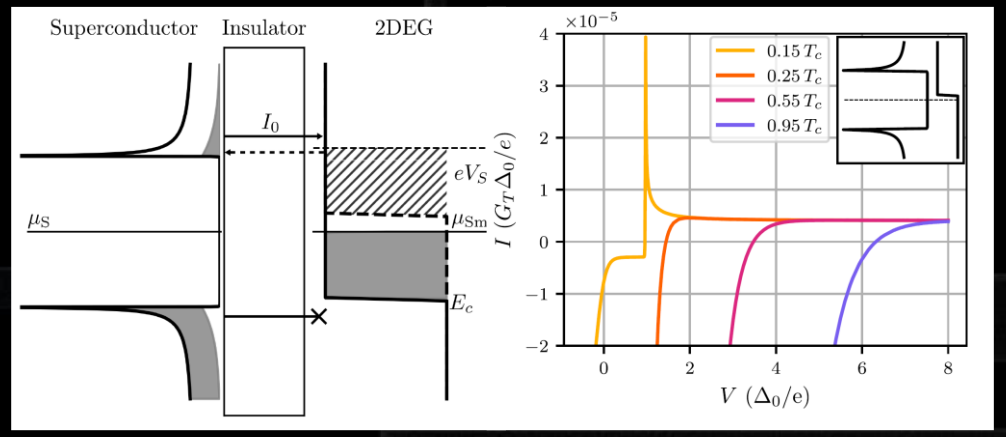

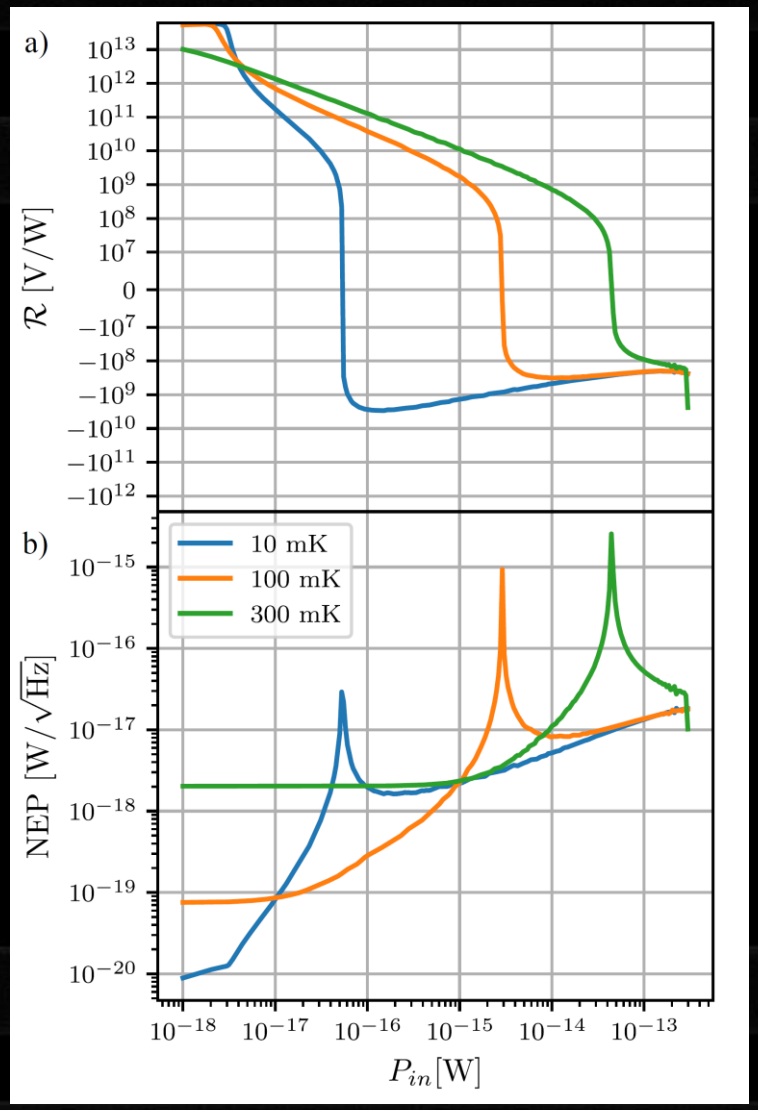

System:

SI2DEG

NEP:

~10^{-20} W/Hz$^{1/2}$

Energy resolution:

ongoing

Time constant:

10^{-6} s

No Josephson coupling

E_C dependent

Need of non-linear model

LL, **FP**, Phys. Rev. B **112**, 184509 (2025)
LL, **FP**, arXiv:2604.02123 (2026)

LL, **FP**, IEEE Trans. Appl. Supercond. (2026)

non-local superconducting detector (NLSD)

NLD: temperature-to-phase conversion

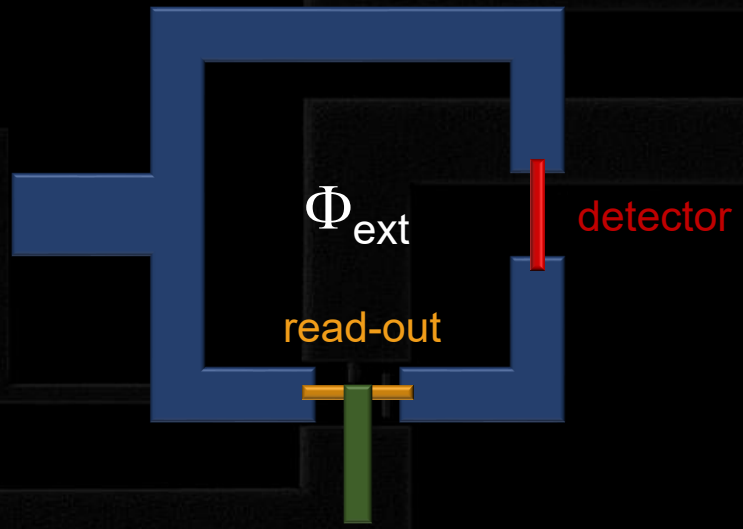

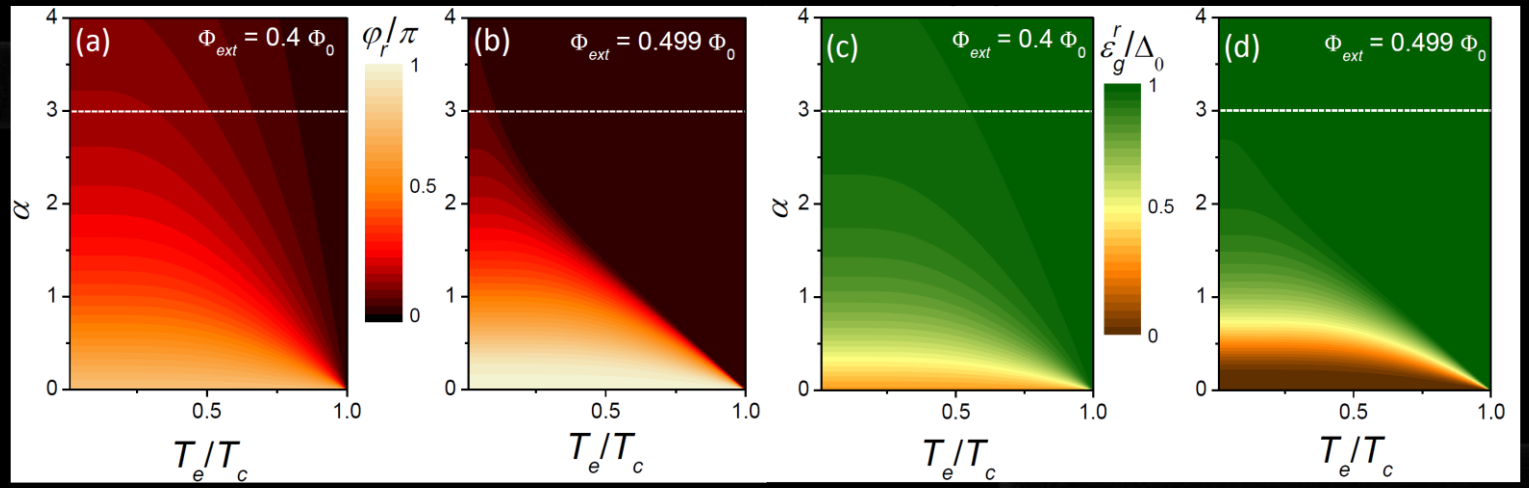

T_e-induced suppression of supercurrent for $\Phi_{ext} \neq 0$

variation finite phase drop across the WLs

conservation of circulating supercurrent

$$I_C^d(T_e, \varphi_d) = I_C^r(T_{bath}, \varphi_r)$$

$$\alpha = \frac{R_N^d}{R_N^r} = \frac{L_J^d}{L_J^r}$$

$$\varepsilon_{gap}^{d,r} = \Delta(T)\cos\left(\varphi_{d,r}/2\right)$$

$\alpha \gg 1$: phase drop across **read-out** JJ

$\alpha \ll 1$: phase drop across **detector** JJ

$\varphi = 0$: gapped metal

$\varphi = \pi$: normal metal

Phys. Rev. Appl. **9**, 054027 (2018)

NLSD: performance

System:
double-loop Josephson interferometer

Quantum-mechanical effect:
macroscopic phase coherence
quantum tunneling

NEP:
ongoing

Energy resolution:
1 GHz

Advantages:
non-locality
in-situ tunable
not affected by de-coherence

Best applications:
dark matter experiments

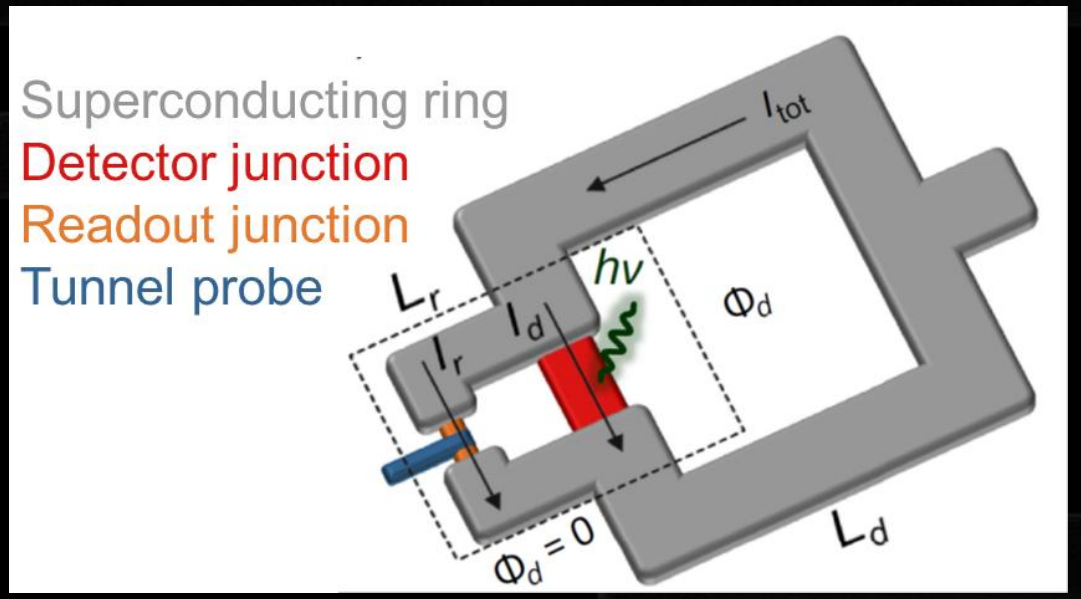

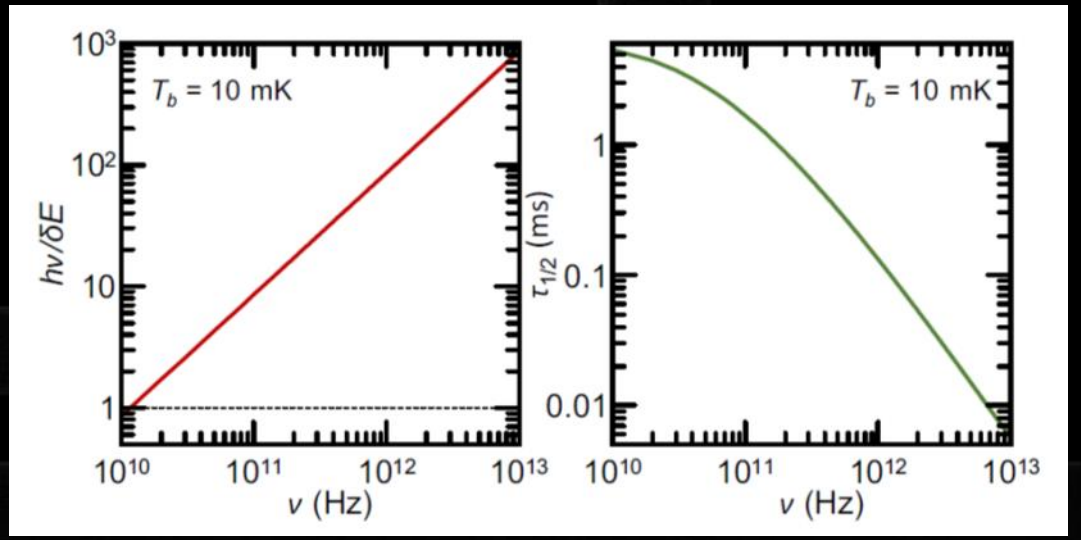

F.P., Phys. Rev. Appl. **20**, 014003 (2023)

NLSD: ongoing activities

Theory

evaluation of the *temperature-to-phase conversion* mechanism in real Josephson interferometers

evaluation of the bolometer response of the NLSD

Experiment

Demonstration of *temperature-to-phase conversion* mechanism

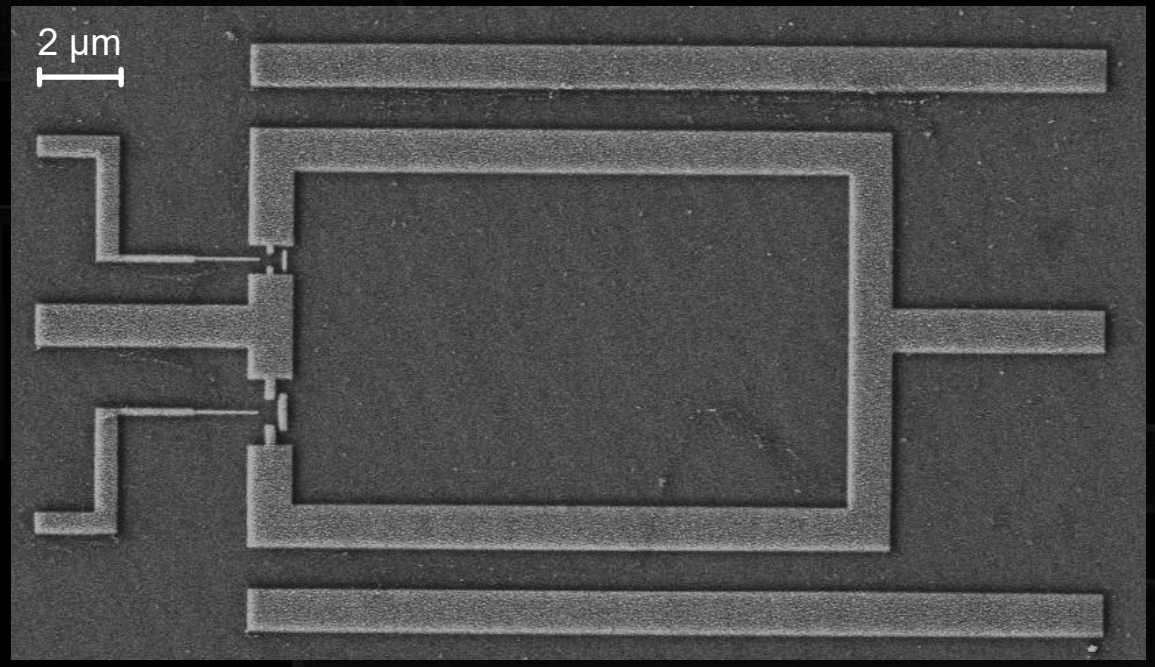

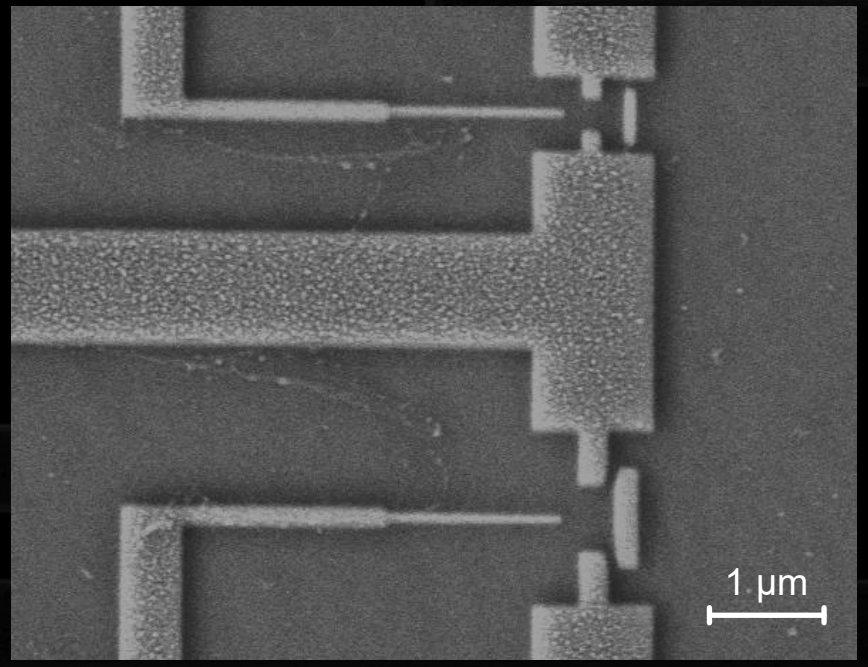

our devices in the technological landscape

Detector	TES	KID	SNSPD	CEB	qubit	JES	NLSD	TED
NEP ($W/Hz^{1/2}$)	10^{-19}	10^{-18}	NO	10^{-18}	NO	10^{-23}	ongoing	10^{-18} ongoing
Min Freq. (Hz)	$5x10^{11}$	$5x10^{11}$	NO (10^{11})	NO	NO (10^{9})	$\sim10^{9}$	$\sim10^{9}$	$\sim10^{9}$

people and fundings

F. Paolucci
L. Lucchesi (post-doc, theory)
L. Vicarelli (post-doc, experiment)
A. Masci (post-doc, experiment)
A. Kotsovolou (PhD, experiment)
M. Cervi (Master, experiment)
R. Balice (Master, experiment)
D. Cecca (Master, experiment)
L. Sassi (Master, experiment)
C. Massai (Master, experiment)

G. Lamanna (University of Pisa)
R. Mannella (University of Pisa)
D. Nicolò (University of Pisa)
A. Pitanti (University of Pisa)
S. Roddaro (University of Pisa)
G. Signorelli (University of Pisa)
A. Tredicucci (University of Pisa)

F. Carillo (INFN Pisa)
C. Puglia (INFN Pisa)
A. Tartari (INFN Pisa)

F. Bianco (CNR-Nano, Pisa, Italy)
F. Giazotto (CNR-Nano, Pisa, Italy)
T. T. Heikkilä (University of Jyväskylä, Jyväskylä, Finland)
J. Meyer (Université Grenoble-Alpes, Grenoble, France)
D. Zhang (Tsinghua University, Beijing China)

MUR FIS2 Call
Project: QuLEAP

INFN CSN V
Project: STEEP

Thank you

back-up slides

why cryogenic systems

At **room temperature**, T_{bath}= 300 K

electron-phonon anelastic scattering

strong energy exchange

$T_e = T_{bath}$

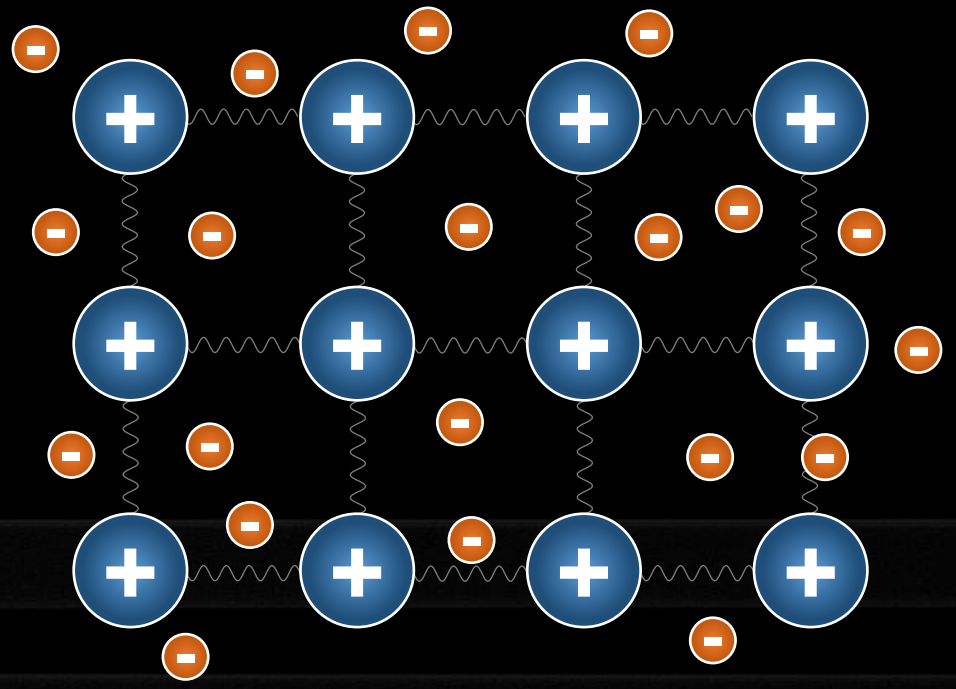

why cryogenic systems

At **cryogenic temperatures**, $T_{bath} < 10$ K

low electron-phonon anelastic scattering

low energy exchange

$T_e \neq T_{bath}$

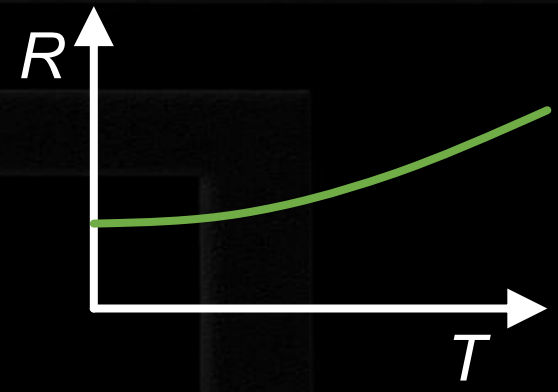

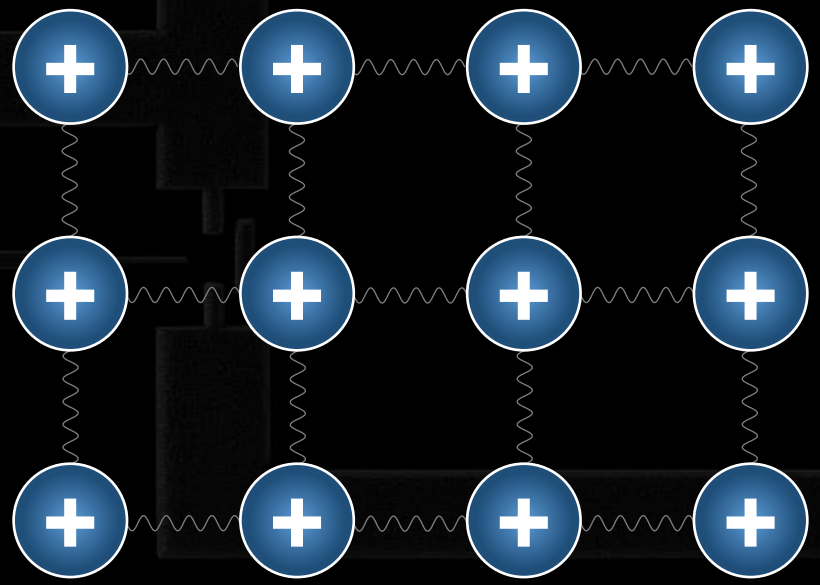

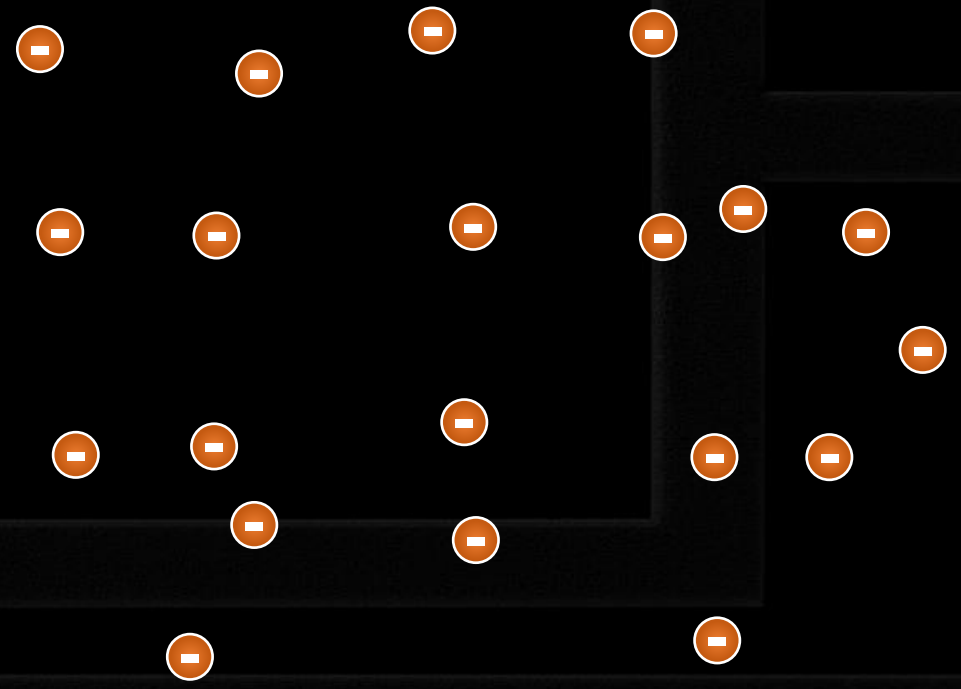

why cryogenic systems

Electron-phonon thermal exchange:

$$\dot{Q}_{e-ph} = -\frac{\Sigma V}{96\zeta(5)k_B^5}\int_{-\infty}^{\infty} dEE\int_{-\infty}^{\infty} d\varepsilon M_{E,E+\varepsilon}(\Delta_{Active}(T), \Gamma_{Active})$$
$$\times \varepsilon|\varepsilon|\left[coth\left(\frac{\varepsilon}{2k_BT_{bath}}\right)(f_E - f_{E+\varepsilon}) - f_E f_{E+\varepsilon} + 1\right]$$

where:

- is the electron-phonon coupling constant;

V is the volume;

$M_{E,E+\varepsilon}$ is a factor depending on the superconducting DOS;

f_E is the difference of Fermi distributions.

In clean metals:

$$\dot{Q}_{e-ph} = \Sigma V\left(T_e^5 - T_{bath}^5\right)$$

Rev. Mod. Phys. **78**, 217 (2006)

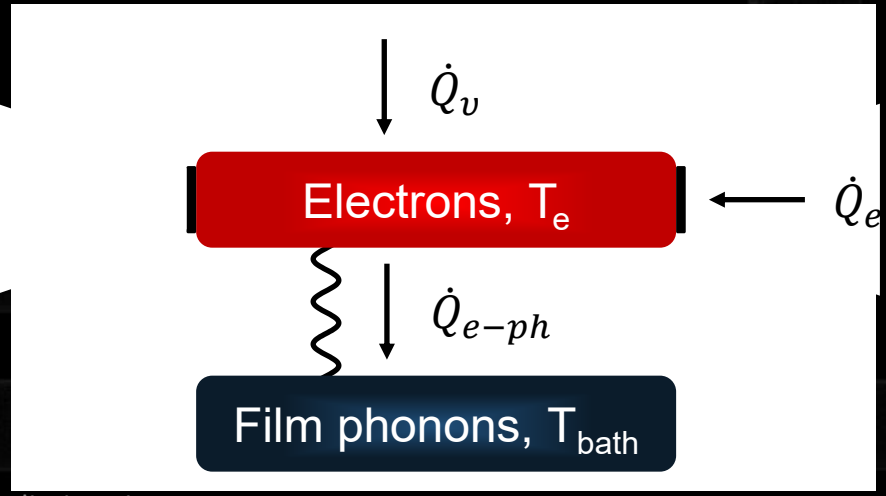

temperatura nei sistemi a stato solido

A **temperature criogeniche**, T_{bath} < 10 K

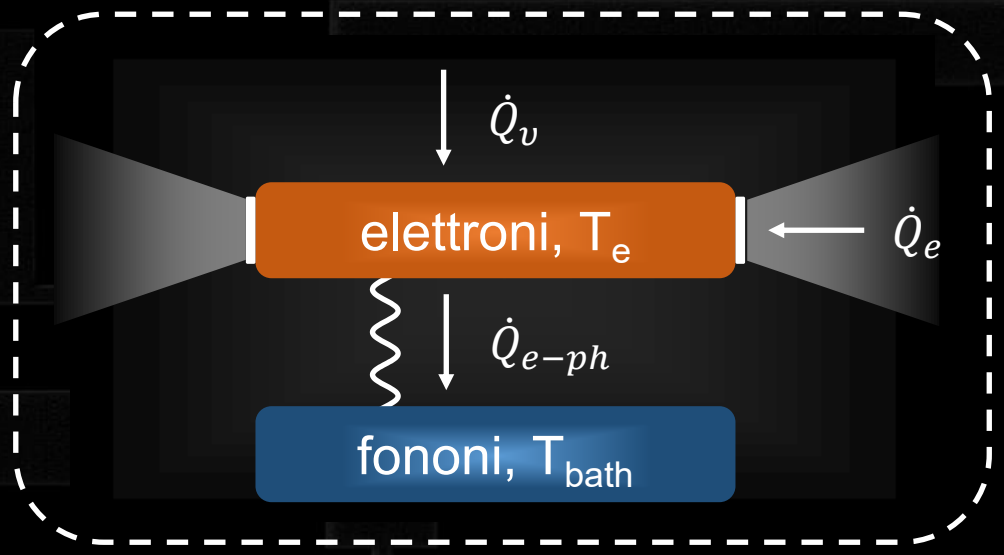

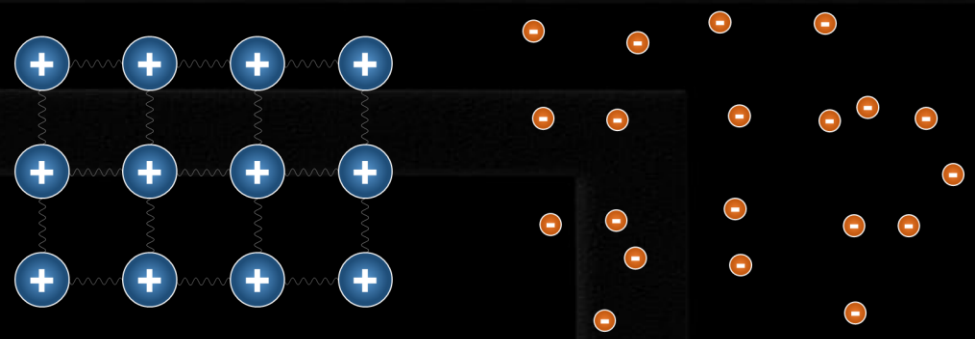

Come varia la temperature?

equazione di bilancio termico

$$\dot{Q}_{e-ph} = \dot{Q}_v + \dot{Q}_e$$

$$\dot{Q}_{e-ph} = \Sigma\mathcal{V}\left(T_e^5 - T_{bath}^5\right)$$

Σ: costante di scattering

$\mathcal{V}$: volume

$\dot{Q}_e$: interazione elettrone-elettrone

$\dot{Q}_v$: interazione elettrone-fotone

minore è $\dot{Q}_{e-ph}$ più la T_e varia facilmente

superconduttività: evidenze sperimentali

Zero resistenza in DC

sotto alla temperature critica, T_C
sotto alla corrente critica, I_C

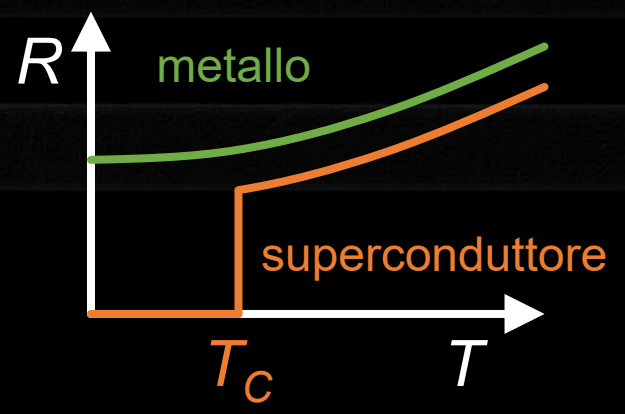

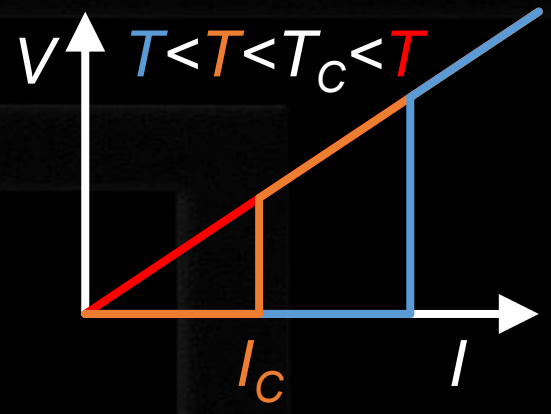

Perfetto diamagnete: espulsione del campo magnetico (effetto Meissner)

sotto alla temperature critica, T_C
sotto al campo magnetico critico, H_C

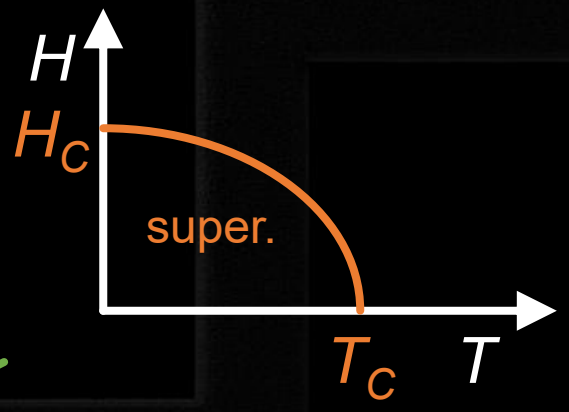

Picco del calore specifico

sotto alla temperature critica, T_C

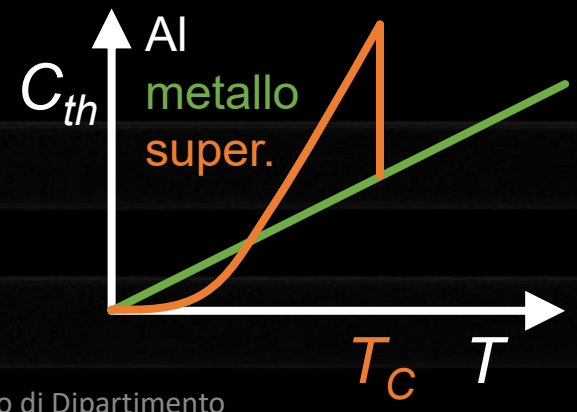

superconduttività: coppie di Cooper

Un elettrone deforma il reticolo

attira leggermente gli ioni positivi: distorsione locale del reticolo

Un secondo elettrone viene attratto

attraverso lo scambio di fononi, due elettroni si attraggono debolmente

Si forma la coppia di Cooper

2 elettroni con spin e momento opposti formano uno stato legato collettivo
la coppia ha momento totale netto zero e si comporta come un unico bosone

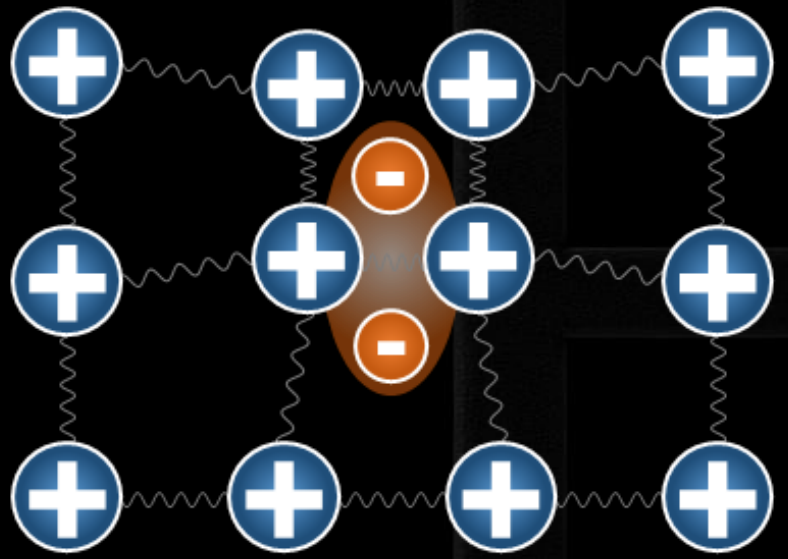

Le coppie di Cooper condensano in un unico stato quantico coerente

superconduttività: gap energetico

Gap superconduttivo: guadagno energetico delle coppie di Cooper sugli elettroni

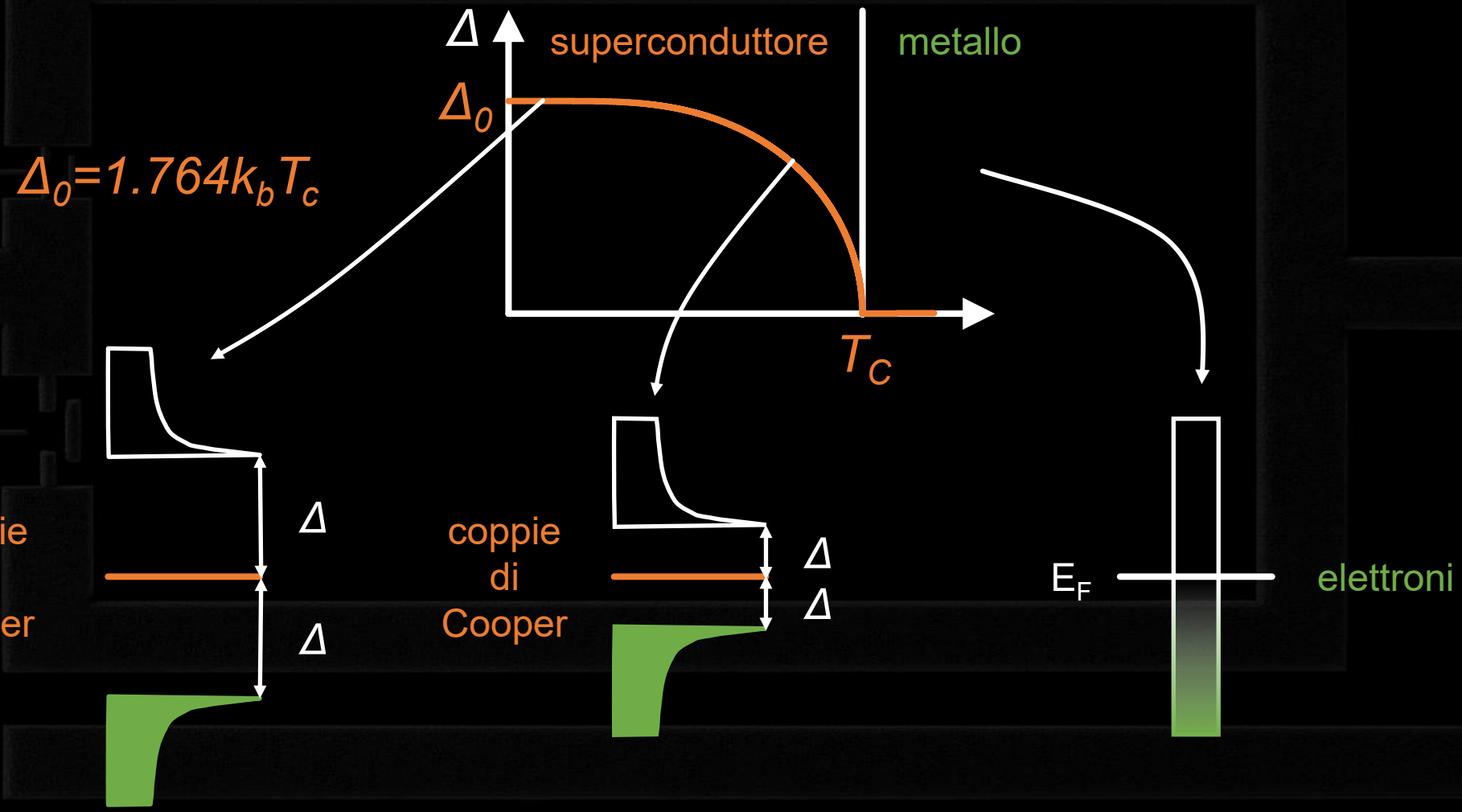

superconduttività: management energetico

Le coppie di Cooper non trasportano calore: isolante termico

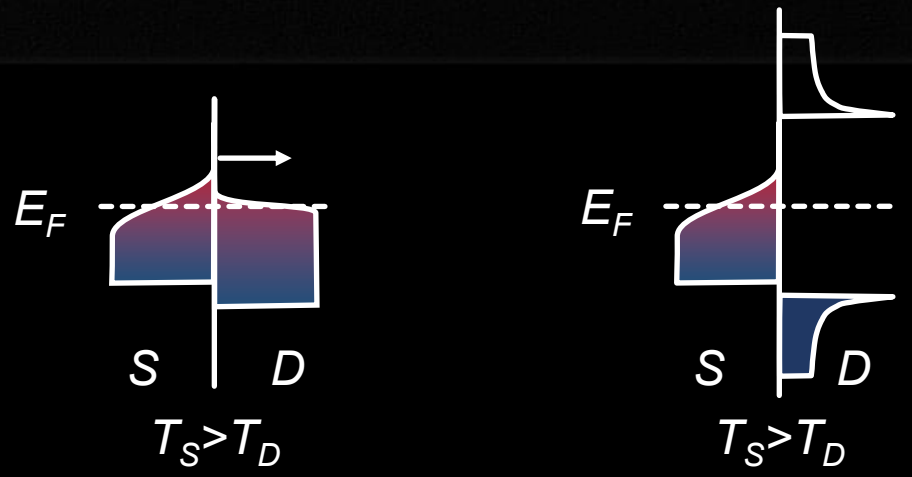

Le coppie di Cooper non termalizzano: facile portare il sistema fuori equilibrio

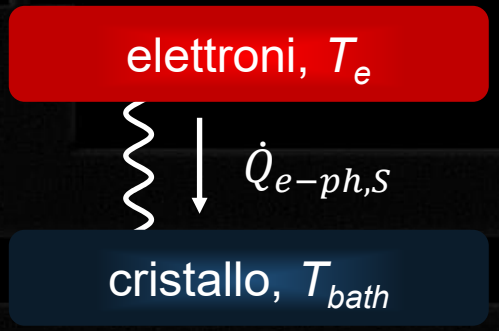

$$\dot{Q}_{e-ph,s} \sim \dot{Q}_{e-ph,m}\, e^{-\frac{\Delta}{k_B T_e}}$$